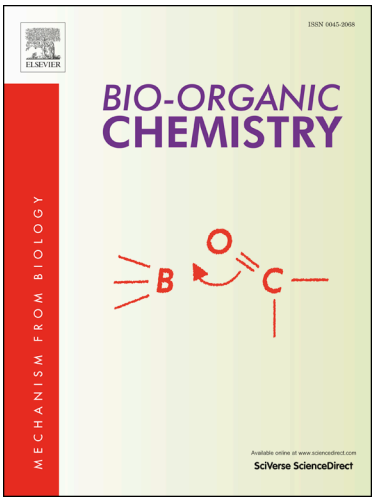

Identification of novel imidazole flavonoids as potent and selective inhibitors of protein tyrosine phosphatase

Ling Zhang, Yu Ge, Qing Ming Wang, Cheng-He Zhou

PII: S0045-2068(18)31472-X
DOI: https://doi.org/10.1016/j.bioorg.2019.03.074
Reference: YBIOO 2900

To appear in: *Bioorganic Chemistry*

Received Date: 14 December 2018
Revised Date: 18 March 2019
Accepted Date: 30 March 2019

Please cite this article as: L. Zhang, Y. Ge, Q. Ming Wang, C-H. Zhou, Identification of novel imidazole flavonoids as potent and selective inhibitors of protein tyrosine phosphatase, *Bioorganic Chemistry* (2019), doi: https://doi.org/10.1016/j.bioorg.2019.03.074

Title page

Title:

Identification of novel imidazole flavonoids as potent and selective inhibitors of protein tyrosine phosphatase

Author names and affiliations:

Ling Zhang[1,*], Yu Ge[1], Qing Ming Wang[1,*] and Cheng-He Zhou[2]

[1,*] *School of Pharmacy, Yancheng Teachers' University, Yancheng, Jiangsu 224051, People's Republic of China*

[2] *Laboratory of Bioorganic & Medicinal Chemistry, School of Chemistry and Chemical Engineering, Southwest University, Chongqing, 400715, P.R. China*

Tel.: 0515-88258905

E-mail: zling891613@163.com (Ling Zhang), wangqm@yctu.edu.cn (Qing Ming Wang)

Abstract:

A series of imidazole flavonoids as new type of protein tyrosine phosphatase inhibitors were synthesized and characterized. Most of them gave potent protein phosphatase 1B (PTP1B) inhibitory activities. Especially, compound **11a** could effectively inhibit PTP1B with an IC_{50} value of 0.63 μM accompanied with high selectivity ratio（9.5-fold) over T-cell protein tyrosine phosphatase (TCPTP). This compound is cell permeable with relatively low cytotoxicity. The high binding affinity and selectivity was disclosed by molecular modeling and dynamics studies. The structural features essential for activity were confirmed by quantum chemical studies.

***Keywords*:**

Flavonoid; Imidazole; Protein tyrosine phosphatase; Selectivity; Cell viability

1. Introduction

Protein tyrosine phosphatases (PTPs) exert an significant effect on catalysis protein tyrosine dephosphorylation and modulation several cellular signal transduction pathways [1]. Dysregulation of PTPs activities causes aberrant tyrosine phosporylation, which lead to the pathogenesis of many human diseases such as cancers, autoimmune disorders, obesity and diabetes [2]. Among the PTPs, PTP1B is a key negative regulator of insulin signaling and acts by directly inactivating insulin receptor (IR) through dephosphorylation tyrosine residues in the regulatory domain [3]. A number of synthetic PTP1B inhibitors have been discovered [4-6]. Compound **1** designed on the basis of catalytic pocket characteristics, was a classic PTP1B inhibitor (IC_{50} = 32 nM) with modest caco-2 permeability, but without selectivity (Figure 1). Compound **2** (IC_{50} = 620 nM) was found to interact with the PTP1B catalytic site Cys215 through establishment of covalent bond, however, the selectivity or membrane permeability was not further reported [7]. PTP inhibitors especially that can inhibit the particular PTP with good permeability are therefore highly desirable [8].

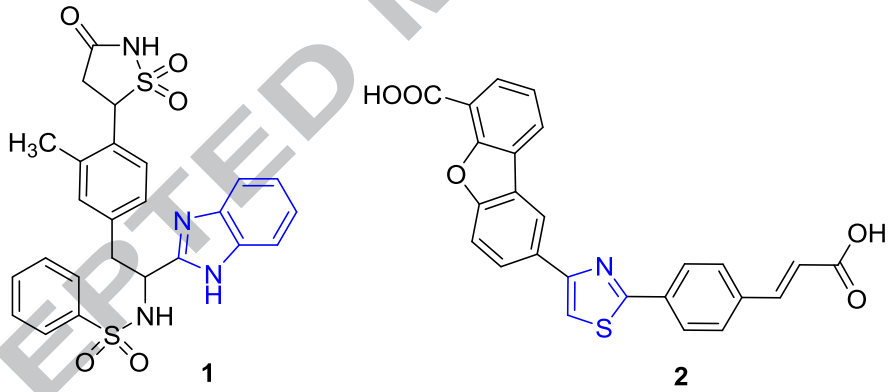

Fig. 1 Some reported PTP1B inhibitors

Chemical modification of biological active compounds of natural origin is one of the most efficient approaches in drug development. Flavonoids with typical benzopyrone framework are a class of plant phenolic compounds that are widely found in fruits, vegetables, seeds and herbs (Figure 2). A large number of studies show that flavonoids exert beneficial effects in the prevention of many diseases, including cancer, cardiovascular disease and neurodegenerative disorders. Specially, some natural flavones extracted from plants and traditional Chinese medicine manifested to be good PTP1B inhibitors due to their low toxicity and high hypoglycemic effects [9]. Especially, they are potentially powerful bioactive agents since it has disclosed that they could selectively inhibit PTP1B activity in a non-competitive way different to the

traditional drugs [10,11], and improve insulin sensitivity in insulin-resistant HepG2 cells *via* the IRS-1/PI3K/AKT pathway [12]. Recently, more and more flavonoids received much attention due to their unique properties in the inhibition of PTP1B (Figure 3).

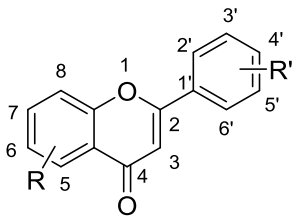

Fig. 2 General structure of flavonoids.

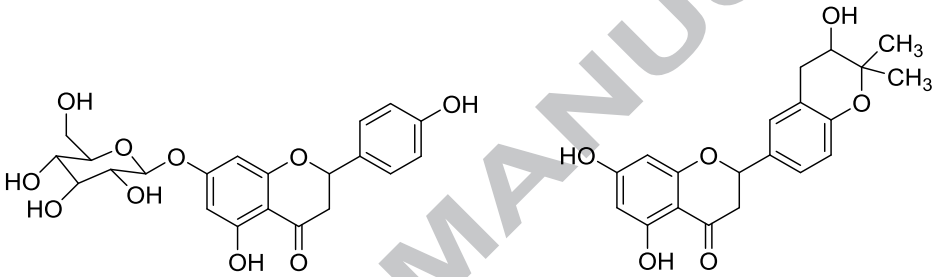

Fig. 3 Some reported flavonoid derivatives as PTP1B inhibitors

Imidazole derivatives has shown large potentiality in medicinal chemistry [13]. The unique structure of imidazole endows its derivatives to readily bind with a variety of enzymes and receptors in biological system via weak interactions such as coordination bonds, hydrogen bonds, ion-dipole, cation-π, π-π stacking, hydrophobic effect, van der Waals force and so on. Literature reported that presence of imidazole ring played an important role to improve the PTP1B inhibitory activity [14,15]. Imidazole derivatives were shown to activate glucose uptake in cell cultures through inhibition of the PTP1B and also demonstrated the inhibition of D-dimer formation, suggesting they could potentially relieve a hypercoagulative state in diabetic patients [16] (Figure 4). This encourages us with special interest to investigate these imidazole compounds as a novel type of PTP1B inhibitors with improved activity.

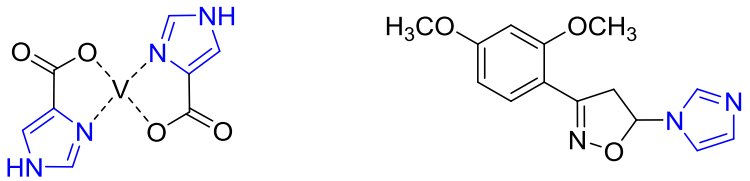

Fig. 4 Some reported imidazole derivatives as PTP1B inhibitors

In recent years, the actual trend in the field of chemistry of flavonoids has been modification by

purposeful introduction into the molecule of nitrogen heterocyclic substituent [17-20]. Such studies are of great interest for the theory of organic synthesis and purposeful synthesis of new biologically active compounds based on flavonoid system. However, much less work has been taken on the synthesis of flavonoids containing nitrogen heterocyclic moiety at C-2 position.

In view of this situation and as an extension of previous work [21,22], it is meaningful for us to combine flavonoids through their C-2 position with different imidazole carbaldehydes to generate a new structural type of potentially PTP1B inhibitors and investigate their effect on the inhibition of PTP1B (Scheme 1).

Since substituents exert big influence on the bioactivities [23-25], various aliphatic chains with different lengths and substituted phenyl moieties containing fluoro, chloro and nitro groups were further modified.

All the synthesized imidazole flavonoids (Scheme 1 and Scheme 2) were characterized and their PTP1B inhibitory activity was also evaluated. The structural features essential for activity were also by investigation of molecular modelling, molecular dynamics, energies and plots of HOMO and LUMO, and plots of MEP.

2 Results and discussion

2.1. Chemistry

The synthetic route of target imidazole flavonoids was outlined in Scheme 1 and Scheme 2. Initially, reactions of compounds **1a–c** with imidazole-4-carbaldehyde afforded the corresponding azoles **2a–c** and **3a–c** in 30.1–53.2% yields (Scheme 1). Possible reactions of imidazole-4-carbaldehyde in the presence of potassium carbonate are shown in Figure 5. In basic conditions, 4-carbaldehyde orientation easily occurred during the *N*-alkylations of imidazole-4-carbaldehyde with alkyl halides. Conversely, the acidic conditions favored the 5-carbaldehyde orientation. Considered the yields were poor under acidic conditions, potassium carbonate was chosen to synthesize the target compounds. Four resonance forms of imidazole-4-carbaldehyde (A–D) exist in basic conditions (Figure 5). Amongst, patterns A and C are more stable than other patterns, so the *N*-1 and *N*-3 alkylated products could be obtained by *N*-alkylation of imidazole-4-carbaldehyde. The *N*-1 alkylated one is predominant due to the relative low acidity of –NH– proton compared to imidazole-5-carbaldehyde. In the preparations of imidazole-4-carbaldehydes **2a–c**, **5a–e,** imidazole-5-carbaldehyde derivatives **3a–c**, **6a–e** were obtained as by-products.

Condensation of 1,3-benzenediol with chloro-acetonitrile in the presence of $ZnCl_2$ in ether was followed by hydrolysis in water and produced ketone **7** in 86% yield [26]. The resulting **7** was reacted with corresponding imidazole carbaldehydes in ethanol with 10% NaOH, was followed by acidification with

aqueous HCl to afford target compounds **8**, **9a–c**, **10a–c**, **11a–e**, and **12a–e** in satisfactory yields.

The alkylation of imidazole-2-carbaldehyde with alkyl halides **1a–c** afforded the corresponding azoles **13a–c** (Scheme 2). *N*-Halobenzyl derivatives **14a–d** were provided in quantitative yields by the reaction of imidazole-2-carbaldehyde with a series of halobenzyl halides **4a–d**. These prepared imidazole halides **13a–c** and **14a–d** respectively were further coupled with ketone **7** to smoothly produce the target imidazole-flavonoid hybrids **15**, **16a–c** and **17a–d**.

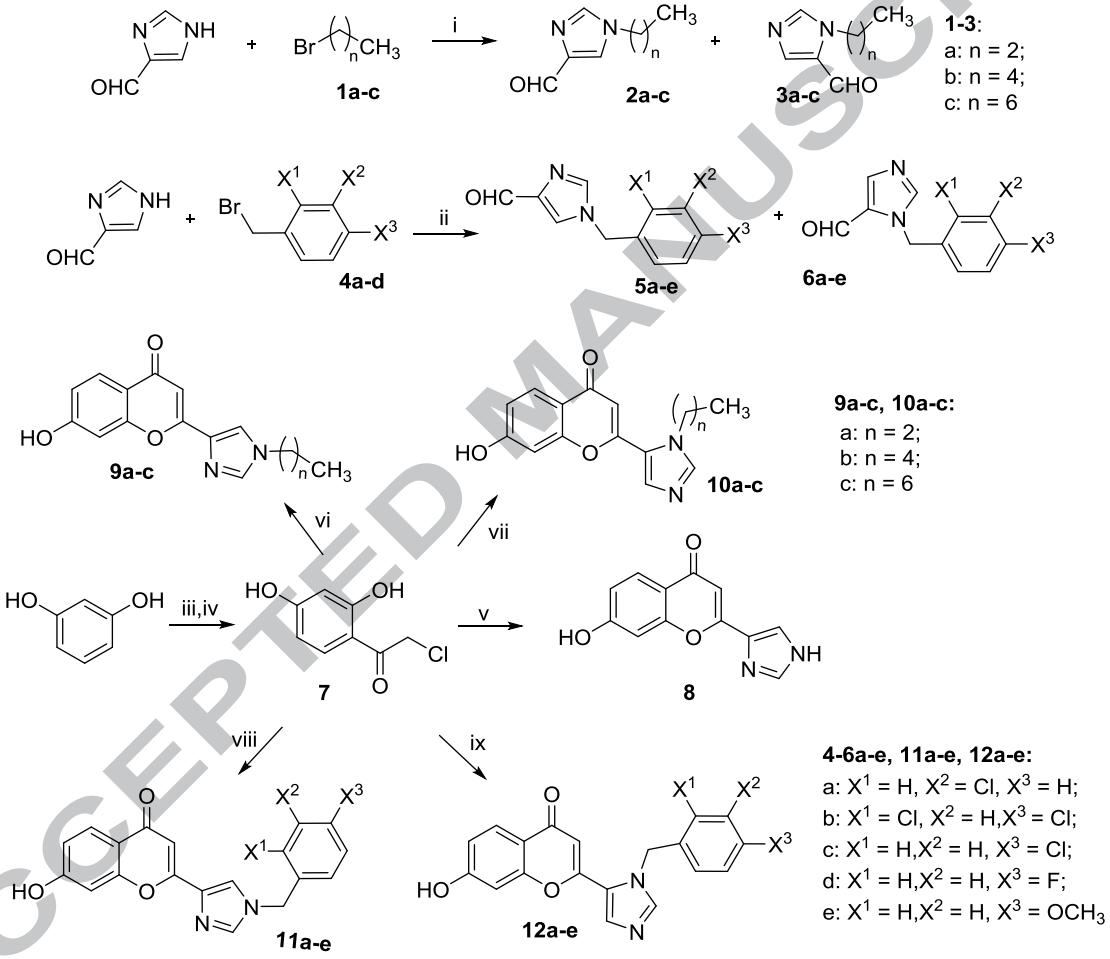

Scheme 1 Synthetic routes of flavonoid imidazoles (I). Reagents and conditions: (i) alkyl bromide, K_2CO_3, EtOH, reflux; (ii) halobenzyl halide, K_2CO_3, EtOH, reflux; (iii) $ClCH_2CN$, EtOEt, HCl (g), 0℃; (iv) 1 mol/L HCl, H_2O, reflux; (v) imidazole-4-carbaldehyde, 10%NaOH, rt, EtOH; (vi) compounds **2a-c**, 10%NaOH, rt, EtOH; (vii) compounds **3a-c**, 10%NaOH, rt, EtOH; (viii) compounds **5a-e**, 10%NaOH, rt, EtOH; (ix) compounds **6a-e**, 10%NaOH, rt, EtOH.

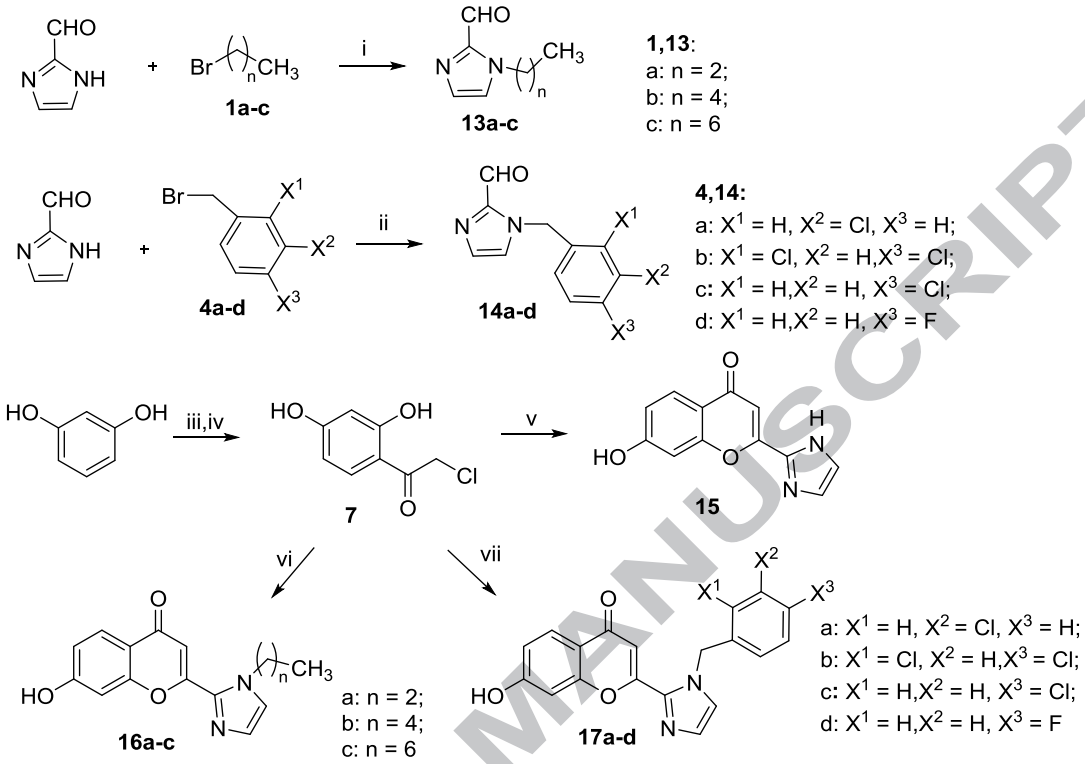

Scheme 2 Synthetic routes of flavonoid imidazoles (II). Reagents and conditions: (i) alkyl bromide, K_2CO_3, EtOH, reflux; (ii) halobenzyl halide, K_2CO_3, EtOH, reflux; (iii) $ClCH_2CN$, EtOEt, HCl (g), 0℃; (iv) 1 mol/L HCl, H_2O, reflux; (v) imidazole-2-carbaldehyde, 10%NaOH, rt, EtOH; (vi) compounds **13a-c**, 10%NaOH, rt, EtOH; (vii) compounds **14a-d**, 10%NaOH, rt, EtOH.

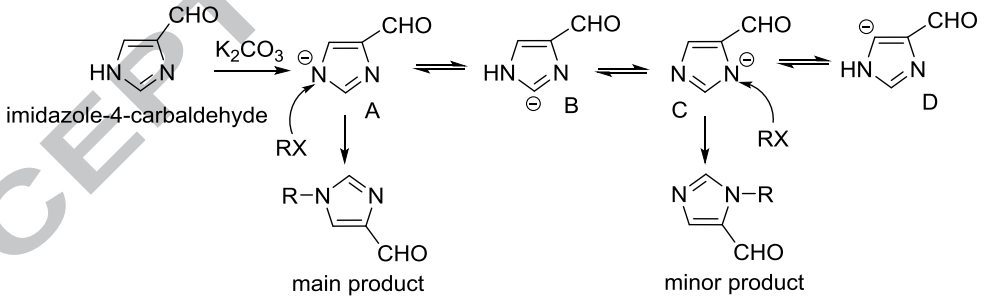

Fig. 5 Possible reactions of imidazole-4-carbaldehyde in the presence of potassium carbonate

2.2. Biological evaluation

2.2.1. Inhibition of phosphatases

The PTP1B inhibitory activity of all the synthesized target compounds **8**, **9a**–**c**, **10a**–**c**, **11a**–**e**, **12a**–**e, 15, 16a**–**c** and **17a**–**e** was evaluated. The results were summarized in Table 1. As illustrated in Table 1, most compounds showed potential inhibitory activities for PTP1B. The results demonstrated that the obvious

effect of the substituents at the imidazoles on biological activity. Moderate PTP1B inhibitory activity was found for most of N-alkyl derivatives **9a**–**c, 10a**–**c** and **16a**–**c**. Amongst, compound **9b** (IC_{50} = 6.3 μmol/L) and **16b** (IC_{50} = 6.0 μmol/L) with pentyl group and **10a** (IC_{50} = 5.0 μmol/L) with propyl group gave the best bioactivity.

Most halobenzyl ones **11a**–**e**, **12a**–**e** and **17a**–**e** exerted relatively better PTP1B inhibitory activities than the alkyl derivatives **9a**–**c**, **10a**–**c** and **16a**–**c**. Notably, in the series of imidazole-4-formyl derivatives, 3-chlorobenzyl hybrid **11a** gave the best anti-PTP1B efficiency with IC_{50} value of 0.63 μmol/L. Besides, compound **11e** with *p*-methoxy group also displayed fairly good activities with the IC_{50} value of 1.0 μmol/L. The replacement of chlorobenzyl moiety by fluorobenzyl group (compound **11d**) resulted in unfavorable potency at the concentrations of 5.0 μmol/L. The positional change of chlorine atom in compound **11a** to give derivatives **11b** and **11c** was not beneficial for the bioactivities.

To our surprise, generally all 5-position substituted imidazoles **10a**–**c**, **12a**–**e** and 2-position substituted imidazoles **15, 16a**–**c** and **17a**–**e** displayed lower anti-PTP1B activities than that of 4-substituted ones **9a**–**c**, **11a**–**e**.

Considered the above discussion, the anti-PTP1B efficacies should be in relation to imidazole ring and halobenzyl group to some extent. For this serial compounds, imidazole-formyl moieties contributed to the anti-PTP1B activities in the order of imidazole-4-formyl derivatives > imidazole-2-formyl derivatives > imidazole-5-formyl ones. The chlorophenyl group was more favorable for improving anti-PTP1B efficacy compared with other benzyl ones.

Table 1 Inhibitory activities against PTP1B (μmol/L)

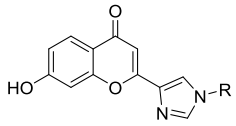
For compounds **8**, **9a-c**, **11a-e**

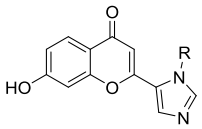
For compounds **10a-c**, **12a-e**

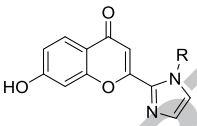
For compounds **15, 16a-c**, **17a-e**

Compounds	IC_{50}	Compounds	IC_{50}	Compounds	IC_{50}
8: R = H	10.0±1.7	**11c**: 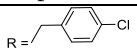	3.1±0.3	**16a**: 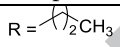	9.8±0.1
9a: 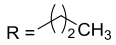	10.0±2.3	**11d**: 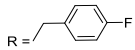	5.0±0.9	**16b**: 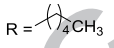	6.0±0.2
9b: 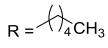	6.3±0.9	**11e**: 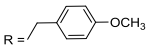	1.0±0.04	**16c**: 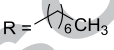	8.2±0.4
9c: 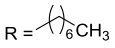	7.9±0.4	**12a**: 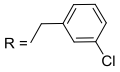	5.0±0.9	**17a**: 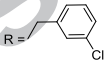	1.1±0.7
10a: 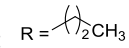	5.0±0.3	**12b**: 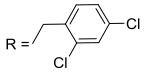	5.0±0.6	**17b**: 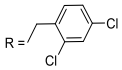	4.1±0.3
10b: 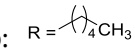	15.0±1.4	**12c**: 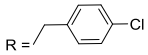	5.0±0.5	**17c**: 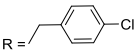	5.0±0.9
10c: 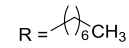	12.5±1.1	**12d**: 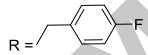	5.0±0.5	**17d**: 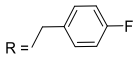	5.7±0.5
11a: 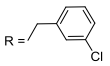	0.63±0.04	**12e**: 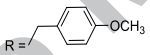	3.1±0.4	**17e**: 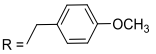	1.2±0.3
11b: 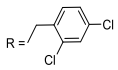	3.9±0.3	**15**: R = H	11.2±0.4	Oleanolic Acid	4.7± 0.2

Further, the selectivity of the **11a** was determined by measuring their inhibitory activity against a panel of several phosphatases including TCPTP, PTP-MEG2 and SHP-2. The IC_{50} values of inhibitor **11a** against the phosphatases, and the selectivity ratios were shown in Table 2. Compound **11a** showed no activity against PTP-MEG2, and only exhibited moderate activity for SHP-2. Obviously, 9.5-fold selectivity for PTP1B over TCPTP was found for compound **11a**.

Table 2 Inhibition of phosphatases by inhibitor **11a**

Compd	IC_{50} (μM)				
	PTP1B	TCPTP	PTP-MEG2	SHP-2	Selective
11a	0.63	5.99	NA	16.87	9.5

[a] NA: no activity
[b] Selective: IC_{50}(TCPTP)/IC_{50}(PTP1B)
[c] Abbreviations: PTP1B, protein tyrosine phosphatase 1B; TCPTP, T-cell protein tyrosine phosphatase; PTP-MEG2, megakaryocyte protein tyrosine phosphatase; SHP-2, src homology phosphatase 2.

2.2.2. Kinetic analysis of PTP1B inhibition

A kinetic analysis of inhibitor **11a** was then performed using *p*-NPP as the substrate. The steady state kinetics assays were conducted under five different concentrations of compound **11a** (0, 1, 2, 4, 8 μM). A competitive inhibition mode versus *p*-NPP was identified since the lines converged at an intersection on the y-axis above the x-axis (Figure 6).

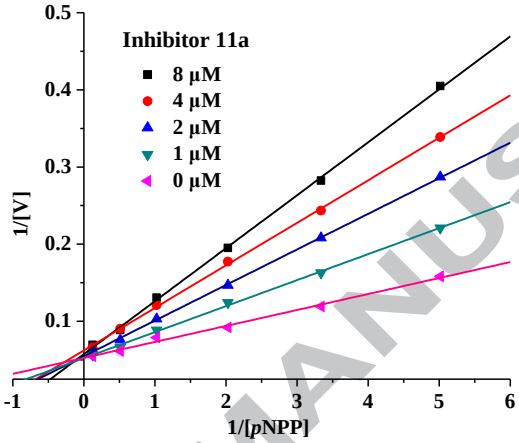

Fig. 6 Compound **11a** is a classical competitive inhibitor

*2.3. The influence of **11a** on cell viability*

Cell Counting Kit-8 (CCK8) method was used to investigate the effect of **11a** on cell viability of HEK293 (human embryonic kidney 293) cells. At high concentration, compound **11a** still gave low toxicity to normal human embryonic kidney cells (Figure 7). The IC_{50} value (324 μg/mL) manifested **11a** has lower cytotoxicity.

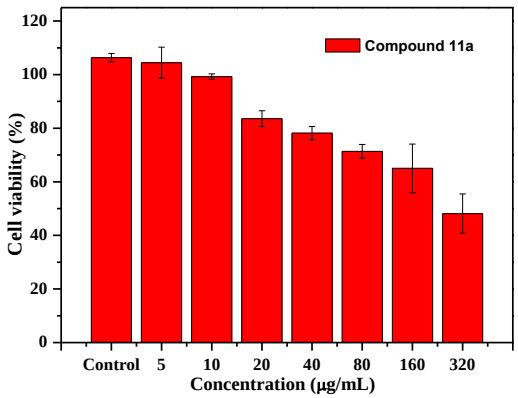

Fig. 7 Relative cell viabilities of compound **11a** in HEK293 cells.

2.3. Molecular modeling

To disclose the observed high binding affinity and selectivity of the target flavonoids, the lowest-energy conformations were calculated by using active site-docking simulations (Figure 8, Supplementary Information: Table S3). The crystal structure data (protein tyrosine phosphatases 1B) were provided by the protein data bank (PDB code: 1T4J). The calculated binding modes of represent compounds in the active site of PTP1B support the bioactivity difference (Table 1) and were illustrated in Figure 8.

According to the docking evaluation, the most active hybrid **11a** (E = -8.78 kJ/mol) with PTP1B might rationalize the possible inhibitory mechanism. The hydroxyl group of this molecule could form hydrogen bonds with Lys197, Glu200 of PTP1B with length of 1.8 Å. Meanwhile, the nitrogen atom of the imidazole moiety and oxygen atom of this molecule could also form hydrogen bonds with the residue Asn193 with length of 2.7 Å and 2.2 Å respectively. These cooperative binding might be beneficial to stabilize the compound-PTP1B enzyme complex, which might be responsible for the good inhibitory efficacy of compound **11a** against PTP1B.

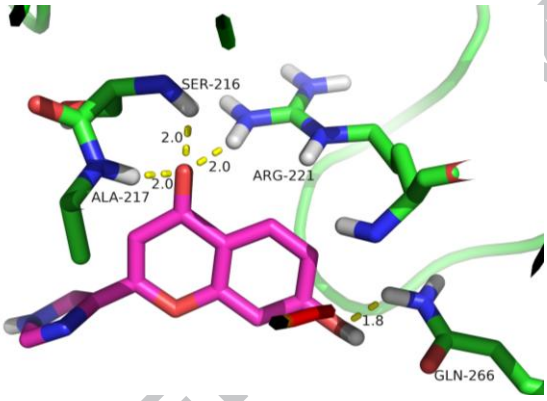

(A) Compound **8** (*E* = -6.94 kJ/mol)

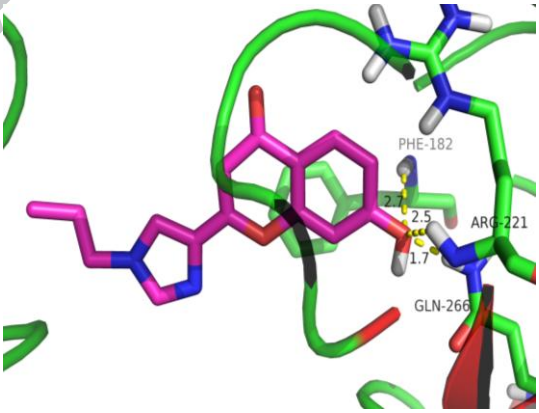

(B) Compound **9a** (*E* = -6.74 kJ/mol)

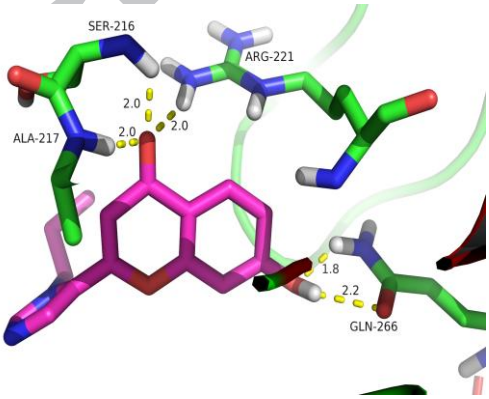

(C) Compound **10a** (*E* = -7.33 kJ/mol)

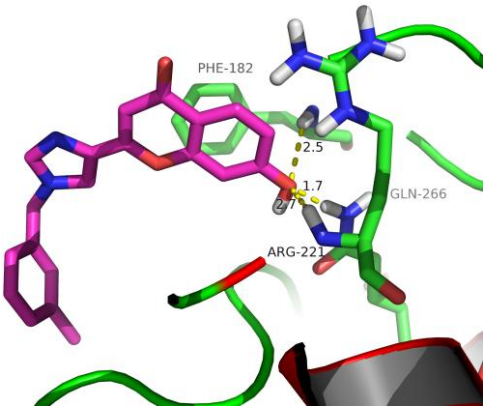

(D) Compound **11a** (*E* = -8.78 kJ/mol)

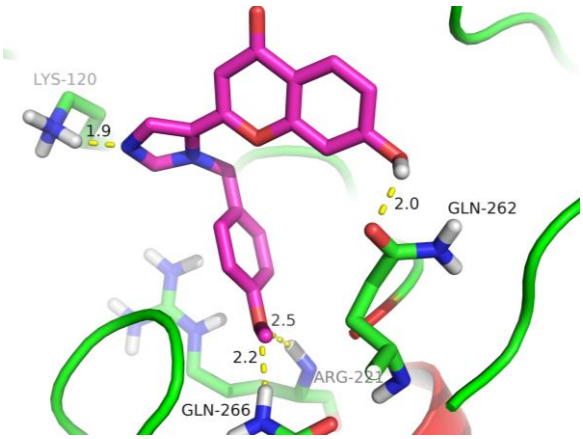

(E) Compound **12e** (*E* = -7.77 kJ/mol)

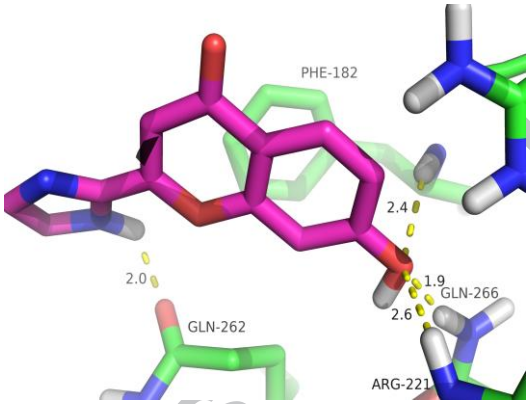

(F) Compound **15** (*E* = -6.34 kJ/mol)

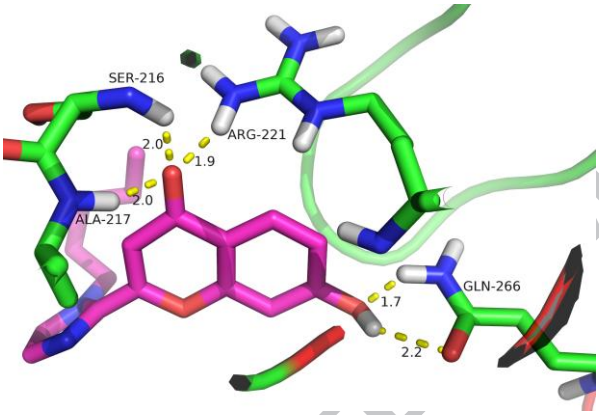

(G) Compound **16b** (*E* = -7.48 kJ/mol)

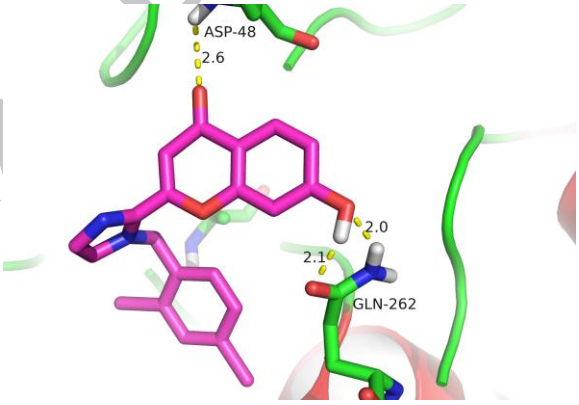

(H) Compound **17b** (*E* = -7.47 kJ/mol)

Fig. 8 Binding modes of all compounds in the active site of PTP1B.

The binding mode of compound **11a** with TCPTP (PDB code: 1L8K) was used to preliminary explain the selectivity of this inhibitor. The main interactions between inhibitor **11a** and the TCPTP was shown in Figure 9. This compound formed hydrogen bonding with amino acid residues Arg-7 with length of 1.7 Å through the oxygen atom. This pattern was different with the binding of **11a** with PTP1B.

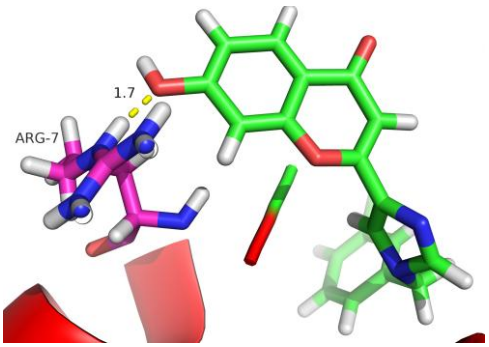

Fig. 9 Three-dimensional conformation of compound **11a** docked onto the active site of TCPTP.

2.4. Analysis of the Dynamics Studies

The interaction of the protein with ligands is a dynamic process. This results in a more stable complex with lower binding energy, and could be displayed by molecular dynamics (MD) simulation.

To analyze the stability of the PTP1B-compound **11a** complex, the root-mean-square deviation (RMSD) values of atoms in PTP1B and PTP1B-compound **11a** complexes were investigated (Figure 10, Supplementary Information: Fig. S1-Fig. S3). The backbone RMSD value of PTP1B was lower than that of TCPTP, which suggested that the PTP1B/**11a** was more stable than TCPTP/**11a** in 50 ns MD simulation (Figure 10, Supplementary Information: Fig. S1-Fig. S3). That may be account for selectivity of PTP1B over TCPTP.

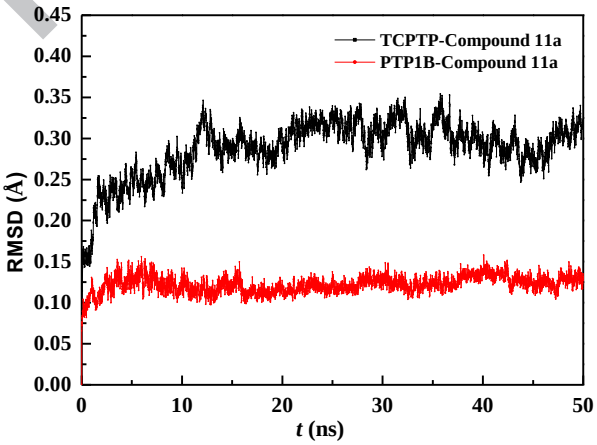

Fig. 10 Time dependence of root-mean-square deviations (RMSD's) for **11a** bound with TCPTP (1L8K, in black) and PTP1B (1T4J, in red)

2.5. Molecular orbital calculation

Electronic effects were shown to be related with biological activity of drugs [27]. At the molecular level,

the frontier molecular orbitals (FMO) controlled the reactivity of a molecule, namely the highest occupied molecular orbital (HOMO) and the lowest unoccupied molecular orbital (LUMO) and they exerted important effect in intermolecular interactions [28]. The extents of these stabilizing interactions in inversely correlation with the energy gap between the interacting orbitals. Higher HOMO energy and lower LUMO energy lead to larger stabilizing interactions, favoring for binding with the receptor. The orbital energies of both HOMO and LUMO and their gaps, were calculated for all the compounds and are shown in Table 3. It is obvious that compounds **9b**, **10a**, **11a**, **11b** and **12e** having the lower energy gap (ΔE) of 1.78, 1.82, 1.99, 1.83 and 1.74 eV, respectively, exhibit the higher bioactivity.

Table 3 Energies of both HOMO and LUMO and their gaps (in eV) calculated for target compounds

Compounds	E_{HOMO}	E_{LUMO}	ΔE
8	-3.210	-1.232	1.98
9a	-2.557	-0.544	2.01
9b	-2.767	-0.985	1.78
9c	-3.156	-1.197	1.96
10a	-2.557	-0.734	1.82
10b	-3.181	-1.116	2.07
10c	-3.178	-1.116	2.06
11a	-3.319	-1.325	1.99
11b	-3.129	-1.306	1.83
11c	-3.292	-1.306	1.99
11d	-3.211	-1.279	1.93
11e	-2.966	-1.034	1.93
12a	-3.401	-1.252	2.15
12b	-3.346	-1.306	2.04
12c	-3.347	-1.279	2.07
12d	-3.293	-1.251	2.04
12e	-2.476	-0.734	1.74
15	-3.374	-0.152	3.22
16a	-3.327	-0.160	3.17
17a	-3.262	-1.308	1.95

Plot of the HOMO and LUMO of the compounds was helpful to determine which atoms were located at the possible sites of electronic transfer between the compound and biological target [29]. The plots of the HOMO and LUMO of all compounds obtained from DFT calculations were obtained (Supplementary Information: Table S1). Some represent compounds are displayed in Figure 11. The results illustrate that HOMO molecular orbital of **8** is mainly located in imidazole ring, indicating the existence of a possible

reactive sites. Therefore, electrophilic attacks might take place on these sites. On the other hand, the LUMO of **8** is primarily concentrated on imidazole and flavonoid rings in which the negatively charged polar residues of the receptor are favorable. Comparing with **8**, the introduction of various substitutions to the imidazole ring produced different characteristic. HOMO of *N*-alkyl derivative **9a** presents similar characteristic, while the LUMO changes significantly. In this case, the LUMO is primarily located in imidazole ring. In contrast, HOMO and LUMO of halobenzyl derivative **11a** presents similar characteristic with compound **8**.

Compounds	HOMO	LUMO
8	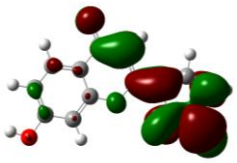	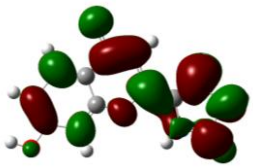
9a	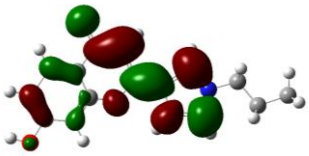	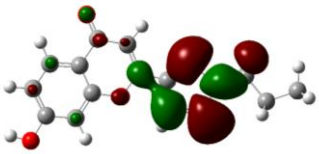
11a	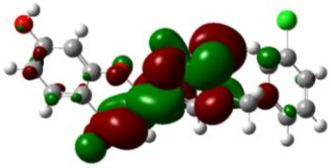	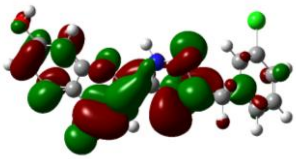

Fig. 11 Plots of the HOMO and LUMO of represent compounds

2.6. Molecular electrostatic potentials

In an attempt to further understand the different bioactivities, molecular electrostatic potentials (MEPs) have been carried out for the lowest energy conformers (Figure 12, Supplementary Information: Table S2). The results show that the nitrogen atom in 1-position of imidazole is more electronically available with the lone pair in unsubstituted imidazole (compound **8, 15** vs **9a, 16b**). Specially, compound **11a** possess increased positive charge regions on the oxygen atoms of OH group. The 5-position substituted imidazoles (**10a**, **12a**, **12b**) possess an increased positive charge regions (in blue) located on the nitrogen atoms of imidazole ring than 4-substituted ones (**9a**, **11a**), which might had unfavorable effects on biological activities.

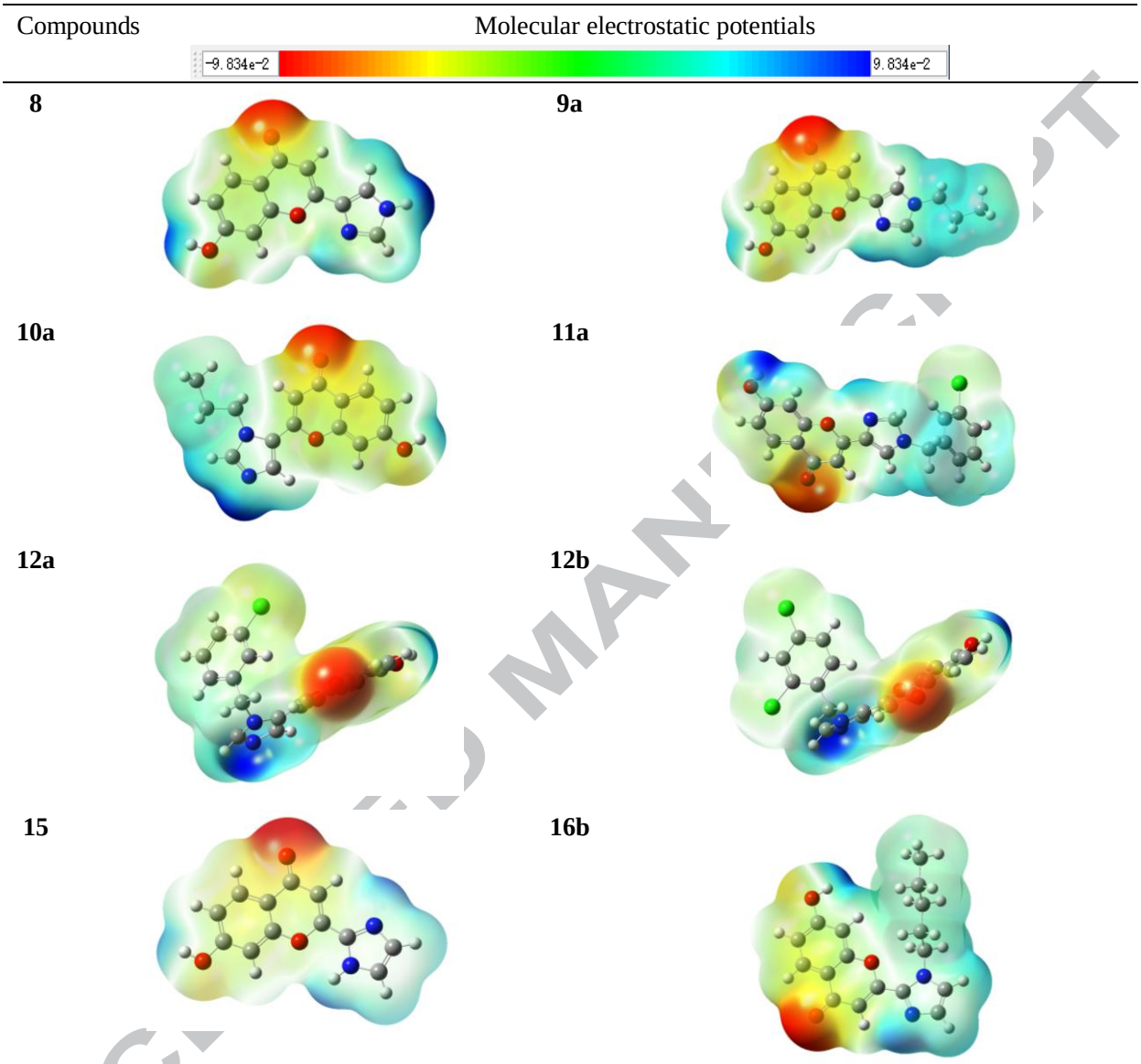

Fig. 12 Molecular electrostatic potentials (MEPs) of represent compounds showing the most positive potential (deepest blue color), the most negative potential (deepest red color), and the intermediate potential (intermediate shades) regions.

3 Conclusion

In conclusion, a series of flavonoid imidazoles were successfully synthesized by a convenient and efficient procedure. Their structures were confirmed by ^{1}H NMR, ^{13}C NMR, MS, IR and HRMS spectra. The *in vitro* protein tyrosine phosphatase inhibition evaluation revealed that most of the synthesized compounds exhibited potent PTP1B inhibitory activities at the micromolar range. The most active

compound **11a** with IC_{50} values of 0.63 μM displayed 9.5-fold selectivity over TCPTP. Molecular modeling studies indicated that the imidazole ring played an important role in the interaction of inhibitor with PTP1B. The MD studies revealed that the PTP1B/**11a** complex was more stable than TCPTP/**11a**, which was the potent proof for observed 9.5-fold selectivity of **11a** for PTP1B over TCPTP. These results provided evidence that flavonoid imidazoles can be potent inhibitors of PTP1B. Further studies on these compounds in cell permeability, selectivity and cellular activity to provide PTP1B inhibitors suitable for *in vivo* proof of animal studies in diabetes are now in progress. All these will be discussed in the future paper.

4 Experimental protocols

4.1 General methods

Melting points were recorded on X-6 melting point apparatus and uncorrected. TLC analysis was done using pre-coated silica gel plates. FT-IR spectra were carried out on Bruker RFS100/S spectrophotometer (Bio-Rad, Cambridge, MA, USA) using KBr pellets in the 400–4000 cm^{-1} range. NMR spectra were recorded on a Bruker AV 300 and 600 spectrometer using TMS as an internal standard. The chemical shifts were reported in parts per million (ppm), the coupling constants (*J*) were expressed in hertz (Hz) and signals were described as singlet (s), doublet (d), triplet (t), as well as multiplet (m). The mass spectra were recorded on LCMS-2010A and the high-resolution mass spectra (HRMS) were recorded on an IonSpec FT-ICR mass spectrometer with ESI resource. All other chemicals and solvents were commercially available, and were used without further purification.

4.2 Synthesis of flavonoid imidazoles

*4.2.1. Synthesis of 1-propyl-1H-imidazole-4-carbaldehyde (**2a**)*

A mixture of imidazole-4-carbaldehyde (0.96 g, 0.01 mol) and potassium carbonate (1.38 g, 0.01 mol) in acetonitrile (5 mL) was stirred at 60 ℃ for 1 h. After the mixture was cooled to room temperature, compound **1a** (2.44 g, 0.02 mol) was added and refluxed for 10 h (monitored by TLC, eluent, ethyl acetate/petroleum, 1:1, v/v). After the solvent was evaporated under reduced pressure, and the resulting residue was extracted with ethyl acetate (3×20 mL), the organic layers were combined, dried over anhydrous sodium sulfate, and concentrated under reduced pressure. The crude product was purified by silica gel column chromatography eluting with ethyl acetate/petroleum (1:2, v/v) to afford the target compound **2a** (0.61 g) as white solid. Yield: 44.1%; mp: 107–108 ℃. ^{1}H NMR (400 MHz, DMSO-d_6) δ: 9.69 (s, 1H, C*H*O), 7.76 (s, 1H, imidazole-2-*H*), 7.52 (s, 1H, imidazole-5-*H*), 3.99 (t, *J* = 7.0 Hz, 2H,

imidazole-CH_2), 1.45 (dd, J = 14.1, 7.0 Hz, 2H, CH_2), 0.75 (t, J = 7.2 Hz, 3H, CH_3) ppm.

*4.2.2. Synthesis of 1-pentyl-1H-imidazole-4-carbaldehyde (**2b**)*

Compound **2b** was prepared according to the procedure described for compound **2a** starting from imidazole-4-carbaldehyde (0.96 g, 0.01 mol), potassium carbonate (1.38 g, 0.01 mol) and compound **1b** (3.02 g, 0.02 mol). The target compound **2b** (0.88 g) was obtained as white solid. Yield: 53.2%; mp: 109–110 °C. ^{1}H NMR (400 MHz, $CDCl_3$) δ: 9.77 (s, 1H, C*H*O), 7.44 (s, 1H, imidazole-2-*H*), 7.27 (s, 1H, imidazole-4-*H*), 3.60 (t, J = 7.2 Hz, 2H, CH_2), 1.81 (d, 2H, CH_2), 1.30 (d, 4H, CH_2CH_2), 0.89 (t, J = 7.0 Hz, 3H, CH_3) ppm.

*4.2.3. Synthesis of 1-heptyl-1H-imidazole-4-carbaldehyde (**2c**)*

Compound **2c** was prepared according to the procedure described for compound **2a** starting from imidazole-4-carbaldehyde (0.96 g, 0.01 mol), potassium carbonate (1.38 g, 0.01 mol) and compound **1c** (3.56 g, 0.02 mol). The target compound **2c** (0.97 g) was obtained as white solid. Yield: 50.1%; mp: 109–110 °C. ^{1}H NMR (600 MHz, DMSO-d_6) δ: 9.75 (s, 1H, C*H*O), 7.72 (s, 1H, imidazole-2-*H*), 7.57 (s, 1H, imidazole-5-*H*), 4.01 (t, J = 7.0 Hz, 2H, imidazole-CH_2), 1.68–1.60 (m, 2H, CH_2), 1.20–1.18 (m, 8H, CH_2), 0.81 (t, J = 7.1 Hz, 3H, CH_3) ppm.

*4.2.4. Synthesis of 1-propyl-1H-imidazole-5-carbaldehyde (**3a**)*

Compound **3a** was prepared according to the procedure described for compound **2a** starting from imidazole-4-carbaldehyde (0.96 g, 0.01 mol), potassium carbonate (1.38 g, 0.01 mol) and compound **1a** (2.44 g, 0.02 mol). The target compound **3a** (0.43 g) was obtained as white solid. Yield: 31.2%; mp: 109–110 °C. ^{1}H NMR (400 MHz, DMSO-d_6) δ: 9.73 (s, 1H, C*H*O), 7.70 (s, 1H, imidazole-2-*H*), 7.63 (d, J = 1.0 Hz, 1H, imidazole-4-*H*), 3.85 (dd, J = 9.3, 4.4 Hz, 2H, imidazole-CH_2), 1.80 (dt, J = 14.1, 7.2 Hz, 2H, CH_2), 0.91–0.89 (m, 3H, CH_3) ppm.

*4.2.5. Synthesis of 1-pentyl-1H-imidazole-5-carbaldehyde (**3b**)*

Compound **3b** was prepared according to the procedure described for compound **2a** starting from imidazole-4-carbaldehyde (0.96 g, 0.01 mol), potassium carbonate (1.38 g, 0.01 mol) and compound **1b** (3.02 g, 0.02 mol). The target compound **3b** (0.53 g) was obtained as white solid. Yield: 32.3%; mp: 106–108 °C. ^{1}H NMR (400 MHz, $CDCl_3$) δ: 9.87 (s, 1H, C*H*O), 7.64 (s, 1H, imidazole-2-*H*), 7.57 (s, 1H, imidazole-4-*H*), 4.00 (t, J = 7.2 Hz, 2H, CH_2), 1.84 (dd, J = 14.8, 7.4 Hz, 2H, CH_2), 1.32 (ddd, J = 15.3,

13.0, 6.2 Hz, 4H, CH_2CH_2), 0.91 (t, *J* = 7.1 Hz, 3H, CH_3) ppm.

*4.2.6. Synthesis of 1-heptyl-1H-imidazole-5-carbaldehyde (**3c**)*

Compound **3c** was prepared according to the procedure described for compound **2a** starting from imidazole-4-carbaldehyde (0.96 g, 0.01 mol), potassium carbonate (1.38 g, 0.01 mol) and compound **1c** (3.56 g, 0.02 mol). The target compound **3c** (0.58 g) was obtained as white solid. Yield: 30.1%; mp: 112–113 ℃. ^{1}H NMR (600 MHz, DMSO-d_6) δ: 9.45 (s, 1H, C*H*O), 7.71 (s, 1H, imidazole-2-*H*), 7.48 (s, 1H, imidazole-4-*H*), 3.83 (t, J = 7.4 Hz, 2H, imidazole-CH_2), 1.63 (dt, J = 12.1, 7.5 Hz, 2H, CH_2), 1.27 (m, 8H, CH_2), 0.83 (t, J = 7.6 Hz, 3H, CH_3) ppm.

*4.2.7. Synthesis of 1-(3-chlorobenzyl)-1H-imidazole-4-carbaldehyde (**5a**)*

Compound **5a** was prepared according to the procedure described for compound **2a** starting from imidazole-4-carbaldehyde (0.96 g, 0.01 mol), potassium carbonate (1.38 g, 0.01 mol) and compound **4a** (4.10 g, 0.02 mol). The target compound **5a** (0.74 g) was obtained as white solid. Yield: 33.6%; mp: 121–122 ℃. ^{1}H NMR (600 MHz, DMSO-d_6) δ: 9.28 (s, 1H, C*H*O), 7.88 (s, 1H, imidazole-2-*H*), 7.65 (s, 1H, imidazole-4-*H*), 7.08 (dd, *J* = 17.0, 5.9 Hz, 2H, Ph-*H*), 6.95 (s, 1H, Ph-2-*H*), 6.70 (d, *J* = 5.3 Hz, 1H, Ph-*H*), 5.35 (s, 2H, CH_2) ppm.

*4.2.8. Synthesis of 1-(2,4-dichlorobenzyl)-1H-imidazole-4-carbaldehyde (**5b**)*

Compound **5b** was prepared according to the procedure described for compound **2a** starting from imidazole-4-carbaldehyde (0.96 g, 0.01 mol), potassium carbonate (1.38 g, 0.01 mol) and compound **4b** (4.79 g, 0.02 mol). The target compound **5b** (0.87 g) was obtained as yellow solid. Yield: 34.2%; mp: 131–132 ℃. ^{1}H NMR (600 MHz, DMSO-d_6) δ: 9.82 (s, 1H, C*H*O), 7.75 (s, 1H, imidazole-2-*H*), 7.62 (s, 1H, imidazole-4-*H*), 7.21 (d, *J* = 6.4 Hz, 1H, Ph-3-*H*), 6.56 (d, *J* = 52.3 Hz, 2H, Ph-5,6-2*H*), 5.35 (s, 2H, CH_2) ppm.

*4.2.9. Synthesis of 1-(4-chlorobenzyl)-1H-imidazole-4-carbaldehyde (**5c**)*

Compound **5c** was prepared according to the procedure described for compound **2a** starting from imidazole-4-carbaldehyde (0.96 g, 0.01 mol), potassium carbonate (1.38 g, 0.01 mol) and compound **4c** (4.10 g, 0.02 mol). The target compound **5c** (0.91 g) was obtained as yellow solid. Yield: 41.2%; mp: 134–135 ℃. ^{1}H NMR (600 MHz, DMSO-d_6) δ: 9.71 (s, 1H, C*H*O), 7.78 (s, 1H, imidazole-2-*H*), 7.67 (s, 1H, imidazole-4-*H*), 7.17 (d, *J* = 8.4 Hz, 2H, Ph-2,6-2*H*), 7.12 (d, *J* = 8.4 Hz, 2H, Ph-3,5-2*H*), 5.50 (s, 2H, CH_2)

ppm.

*4.2.10. Synthesis of 1-(4-fluorobenzyl)-1H-imidazole-4-carbaldehyde (**5d**)*

Compound **5d** was prepared according to the procedure described for compound **2a** starting from imidazole-4-carbaldehyde (0.96 g, 0.01 mol), potassium carbonate (1.38 g, 0.01 mol) and compound **4d** (4.10 g, 0.02 mol). The target compound **5d** (0.65 g) was obtained as yellow solid. Yield: 32.0%; mp: 134–135 °C. ^{1}H NMR (400 MHz, $CDCl_3$) δ: 9.75 (s, 1H, C*H*O), 7.56 (s, 1H, imidazole-3-*H*), 7.54 (s, 1H, imidazole-5-*H*), 7.13 (dd, *J* = 8.4, 5.2 Hz, 2H, Ph-2,6-2*H*), 6.99 (dd, *J* = 9.4, 7.7 Hz, 2H, Ph-3,5-2*H*), 5.09 (s, 2H, CH_2) ppm.

*4.2.11. Synthesis of 1-(4-methoxybenzyl)-1H-imidazole-4-carbaldehyde (**5e**)*

Compound **5e** was prepared according to the procedure described for compound **2a** starting from imidazole-4-carbaldehyde (0.96 g, 0.01 mol), potassium carbonate (1.38 g, 0.01 mol) and compound **4e** (4.02 g, 0.02 mol). The target compound **5e** (0.59 g) was obtained as yellow solid. Yield: 27.2%; mp: 134–135 °C. ^{1}H NMR (400 MHz, $CDCl_3$) δ: 9.75 (s, 1H, C*H*O), 7.56 (s, 1H, imidazole-3-*H*), 7.54 (s, 1H, imidazole-5-*H*), 7.13 (dd, *J* = 8.4, 5.2 Hz, 2H, Ph-2,6-2*H*), 6.99 (dd, *J* = 9.4, 7.7 Hz, 2H, Ph-3,5-2*H*), 5.09 (s, 2H, CH_2) ppm.

*4.2.12. Synthesis of 1-(3-chlorobenzyl)-1H-imidazole-5-carbaldehyde (**6a**)*

Compound **6a** was prepared according to the procedure described for compound **2a** starting from imidazole-4-carbaldehyde (0.96 g, 0.01 mol), potassium carbonate (1.38 g, 0.01 mol) and compound **4a** (4.10 g, 0.02 mol). The target compound **6a** (0.82 g) was obtained as white solid. Yield: 37.1%; mp: 123–124 °C. ^{1}H NMR (600 MHz, DMSO-d_6) δ: 9.81 (s, 1H, C*H*O), 7.83 (s, 1H, imidazole-2-*H*), 7.75 (s, 1H, imidazole-4-*H*), 7.00 (dd, *J* = 16.1, 7.5 Hz, 2H, Ph-*H*), 6.91 (s, 1H, Ph-2-*H*), 6.80 (d, *J* = 7.5 Hz, 1H, Ph-*H*), 5.31 (s, 2H, CH_2) ppm.

*4.2.13. Synthesis of 1-(2,4-dichlorobenzyl)-1H-imidazole-5-carbaldehyde (**6b**)*

Compound **6b** was prepared according to the procedure described for compound **2a** starting from imidazole-4-carbaldehyde (0.96 g, 0.01 mol), potassium carbonate (1.38 g, 0.01 mol) and compound **4b** (4.79 g, 0.02 mol). The target compound **6b** (0.91 g) was obtained as yellow solid. Yield: 35.5%; mp: 134–135 °C. ^{1}H NMR (600 MHz, DMSO-d_6) δ: 9.74 (s, 1H, C*H*O), 7.86–7.72 (m, 2H, imidazole-2-*H*, imidazole-4-*H*), 7.18 (d, *J* = 7.3 Hz, 1H, Ph-3-*H*), 6.78 (dd, *J* = 8.5, 2.3 Hz, 1H, Ph-5-*H*), 6.70 (d, *J* = 8.5 Hz, 1H,

Ph-6-*H*), 5.30 (s, 2H, CH_2) ppm.

*4.2.14. Synthesis of 1-(4-chlorobenzyl)-1H-imidazole-5-carbaldehyde (**6c**)*

Compound **6c** was prepared according to the procedure described for compound **2a** starting from imidazole-4-carbaldehyde (0.96 g, 0.01 mol), potassium carbonate (1.38 g, 0.01 mol) and compound **4c** (4.10 g, 0.02 mol). The target compound **6c** (0.86 g) was obtained as yellow solid. Yield: 39.2%; mp: 131–132 °C. ^{1}H NMR (600 MHz, DMSO-d_6) δ: 9.76 (s, 1H, C*H*O), 7.83 (d, *J* = 7.2 Hz, 2H, imidazole-2-*H*, imidazole-4-*H*), 7.46 (d, *J* = 8.1 Hz, 2H, Ph-2,6-2*H*), 7.16 (d, *J* = 8.1 Hz, 2H, Ph-3,5-2*H*), 5.13 (s, 2H, CH_2) ppm.

*4.2.15. Synthesis of 1-(4-fluorobenzyl)-1H-imidazole-5-carbaldehyde (**6d**)*

Compound **6d** was prepared according to the procedure described for compound **2a** starting from imidazole-4-carbaldehyde (0.96 g, 0.01 mol), potassium carbonate (1.38 g, 0.01 mol) and compound **4d** (4.10 g, 0.02 mol). The target compound **6d** (0.66 g) was obtained as yellow solid. Yield: 32.4%; mp: 134–135 °C. ^{1}H NMR (400 MHz, $CDCl_3$) δ: 9.76 (s, 1H, C*H*O), 7.84 (s, 1H, imidazole-2-*H*), 7.73 (s, 1H, imidazole-4-*H*), 7.28–7.19 (m, 2H, Ph-2,6-2*H*), 7.04 (t, *J* = 8.4 Hz, 2H, Ph-3,5-2*H*), 5.49 (s, 2H, CH_2) ppm.

*4.2.16. Synthesis of 1-(4-methoxybenzyl)-1H-imidazole-5-carbaldehyde (**6e**)*

Compound **6e** was prepared according to the procedure described for compound **2a** starting from imidazole-4-carbaldehyde (0.96 g, 0.01 mol), potassium carbonate (1.38 g, 0.01 mol) and compound **4e** (4.02 g, 0.02 mol). The target compound **6e** (0.74 g) was obtained as yellow solid. Yield: 34.2%; mp: 137–138 °C. ^{1}H NMR (600 MHz, DMSO-d_6) δ: 9.82 (s, 1H, C*H*O), 7.74 (d, *J* = 15.2 Hz, 2H, imidazole-2-*H*, imidazole-5-*H*), 7.13 (d, *J* = 8.3 Hz, 2H, Ph-2,6-2*H*), 6.75 (d, *J* = 8.3 Hz, 2H, Ph-3,5-2*H*), 5.34 (s, 2H, CH_2), 3.54 (s, 3H, CH_3) ppm.

*4.2.17. Synthesis of 7-hydroxy-2-(1H-imidazol-4-yl)-4H-chromen-4-one (**8**)*

To a mixture of acetophenone **7** (0.56 g, 3.0 mmol) and imidazole-4-carbaldehyde (0.29 g, 3.0 mmol) in ethanol (25 mL) was added 10% sodium hydrate aqueous (5 mL), the mixture was stirred for 24 h at room temperature[17]. The solution was acidified with 1N HCl and filtered, and the filter cake was recrystallized from ethanol got **8** as white power (0.60 g). Yield: 87.4%; mp: 185–186 °C; IR (KBr, cm^{-1}) ν: 3443 (OH), 3063 (Ar–H), 1719 (C=O), 1617, 1571 (aromatic frame); ^{1}H NMR (400 MHz, DMSO-d_6) δ: 11.44 (s, 1H, O*H*), 7.91 (s, 1H, imidazole-2-*H*), 7.79 (s, 1H, imidazole-5-*H*), 7.59 (d, *J* = 8.4 Hz, 1H, flavone-5-*H*), 6.85

(d, *J* = 1.8 Hz, 1H, flavone-3-*H*), 6.77–6.72 (m, 2H, flavone-6-*H*, flavone-8-*H*) ppm; ^{13}C NMR (101 MHz, DMSO-d_6) δ: 181.2, 167.7, 166.9, 146.0, 138.0, 130.6, 126.0, 113.9, 113.3, 104.1, 99.0 ppm; MS (m/z): 229 $[M+H]^+$; HRMS (TOF) calcd for $C_{12}H_8N_2O_3$: $[M+H]^+$, 229.0613; found, 229.0617.

*4.2.18. Synthesis of 7-hydroxy-2-(1-propyl-1H-imidazol-4-yl)-4H-chromen-4-one (**9a**)*

Compound **9a** was prepared according to the procedure described for compound **8** starting from acetophenone **7** (0.56 g, 3.0 mmol) and compound **2a** (0.41 g, 3.0 mmol). The target compound **9a** (0.52 g) was obtained as white solid. Yield: 64.0%; mp: 201–202 ℃; IR (KBr, cm^{-1}) ν: 3464 (OH), 3050 (Ar–H), 1723 (C=O), 1619, 1543, 1481 (aromatic frame); ^{1}H NMR (400 MHz, DMSO-d_6) δ: 7.96 (s, 1H, imidazole-2-*H*), 7.75 (s, 1H, imidazole-5-*H*), 7.54 (d, *J* = 8.5 Hz, 1H, flavone-5-*H*), 6.81 (d, *J* = 1.9 Hz, 1H, flavone-3-*H*), 6.71 (d, *J* = 2.0 Hz, 1H, flavone-6-*H*), 6.69 (s, 1H, flavone-8-*H*), 4.10 (t, *J* = 7.1 Hz, 2H, imidazole-CH_2), 1.64 (dd, *J* = 14.4, 7.3 Hz, 2H, CH_2), 0.78 (t, *J* = 7.4 Hz, 3H, CH_3) ppm; ^{13}C NMR (101 MHz, DMSO-d_6) δ: 180.9, 167.7, 167.1, 146.8, 140.9, 135.0, 126.1, 125.1, 113.6, 99.2, 97.6, 46.2, 24.3, 11.2 ppm; MS (m/z): 271 $[M+H]^+$; HRMS (TOF) calcd for $C_{15}H_{14}N_2O_3$: $[M+H]^+$, 271.1083; found, 271.1082.

*4.2.19. Synthesis of 7-hydroxy-2-(1-pentyl-1H-imidazol-4-yl)-4H-chromen-4-one (**9b**)*

Compound **9b** was prepared according to the procedure described for compound **8** starting from acetophenone **7** (0.56 g, 3.0 mmol) and compound **2b** (0.50 g, 3.0 mmol). The target compound **9b** (0.53 g) was obtained as white solid. Yield: 60.4%; mp: 191–192 ℃; IR (KBr, cm^{-1}) ν: 3458 (OH), 3060 (Ar–H), , 1717 (C=O), 1624, 1536, 1473 (aromatic frame); ^{1}H NMR (600 MHz, DMSO-d_6) δ: 11.44 (s, 1H, O*H*), 7.93 (s, 1H, imidazole-2-*H*), 7.77 (s, 1H, imidazole-5-*H*), 7.60 (d, J = 8.5 Hz, 1H, flavone-5-*H*), 6.87 (s, 1H, flavone-3-*H*), 6.77 (dd, J = 8.5, 1.6 Hz, 1H, flavone-6-*H*), 6.74 (s, 1H, flavone-8-*H*), 4.18 (t, J = 7.1 Hz, 2H, imidazole-CH_2), 1.68 (dt, J = 14.7, 7.3 Hz, 2H, CH_2), 1.29 (dt, J = 14.0, 6.9 Hz, 2H, CH_2), 1.21 (dd, J = 15.1, 6.9 Hz, 2H, CH_2), 0.85 (t, J = 7.3 Hz, 3H, CH_3) ppm; ^{13}C NMR (151 MHz, DMSO-d_6) δ: 180.9, 167.8, 167.0, 141.2, 135.8, 126.0, 125.0, 113.5-113.4, 99.1, 97.7, 44.6, 31.6, 31.0, 28.5, 26.2, 22.4, 14.3 ppm; MS (m/z): 299 $[M+H]^+$; HRMS (TOF) calcd for $C_{17}H_{18}N_2O_3$: $[M+H]^+$, 299.1396; found, 299.1400.

*4.2.20. Synthesis of 2-(1-heptyl-1H-imidazol-4-yl)-7-hydroxy-4H-chromen-4-one (**9c**)*

Compound **9c** was prepared according to the procedure described for compound **8** starting from acetophenone **7** (0.56 g, 3.0 mmol) and compound **2c** (0.58 g, 3.0 mmol). The target compound **9b** (0.56 g) was obtained as white solid. Yield: 57.4%; mp: 107–108 ℃; IR (KBr, cm^{-1}) ν: 3443 (OH), 3030 (Ar–H), 1714 (C=O), 1638, 1545, 1499, 1458 (aromatic frame); ^{1}H NMR (600 MHz, DMSO-d_6) δ:11.33 (s, 1H,

O*H*), 7.92 (s, 1H, imidazole-2-*H*), 7.77 (s, 1H, imidazole-5-*H*), 7.60 (d, *J* = 8.4 Hz, 1H, flavone-5-*H*), 6.85 (d, *J* = 1.8 Hz, 1H, flavone-3-*H*), 6.76 (d, *J* = 1.9 Hz, 1H, flavone-6-*H*), 6.74 (s, 1H, flavone-8-*H*), 4.17 (t, *J* = 7.1 Hz, 2H, imidazole-CH_2), 1.71–1.63 (m, 2H, CH_2), 1.27–1.21 (m, 8H, CH_2), 0.84 (t, *J* = 7.0 Hz, 3H, CH_3) ppm; ^{13}C NMR (151 MHz, DMSO-d_6) δ: 180.6–180.5, 168.0–167.8, 147.0, 141.6, 135.7, 134.2, 133.7, 133.0–132.8, 129.6, 97.0–96.8 ppm; MS (m/z): 327 $[M+H]^+$. HRMS (TOF) calcd for $C_{19}H_{22}N_2O_3$: $[M+H]^+$, 327.1709; found, 327.1714.

*4.2.21. Synthesis of 7-hydroxy-2-(1-propyl-1H-imidazol-5-yl)-4H-chromen-4-one (**10a**)*

Compound **10a** was prepared according to the procedure described for compound **8** starting from acetophenone **7** (0.56 g, 3.0 mmol) and compound **3a** (0.41 g, 3.0 mmol). The target compound **10a** (0.52 g) was obtained as white solid. Yield: 62.0%; mp: 203–205 ℃; IR (KBr, cm^{-1}) ν: 3432 (OH), 3020 (Ar–H), 1716 (C=O), 1615, 1549, 1483 (aromatic frame); ^{1}H NMR (400 MHz, DMSO-d_6) δ: 11.18 (s, 1H, O*H*), 7.90 (s, 1H, imidazole-2-*H*), 7.83 (d, *J* = 1.0 Hz, 1H, imidazole-4-*H*), 7.59 (dd, *J* = 8.4, 2.9 Hz, 1H, flavone-5-*H*), 6.78 (d, *J* = 1.9 Hz, 1H, flavone-3-*H*), 6.73–6.70 (m, 1H, flavone-6-*H*), 6.65 (s, 1H, flavone-8-*H*), 4.03 (dd, *J* = 9.5, 4.6 Hz, 2H, imidazole-CH_2), 1.80 (dt, *J* = 14.3, 7.3 Hz, 2H, CH_2), 0.88–0.83 (m, 3H, CH_3) ppm; ^{13}C NMR (101 MHz, DMSO-d_6) δ: 181.2, 167.7, 166.6, 146.0, 139.4, 134.1, 126.1, 125.0, 114.0, 113.2, 106.3, 98.9, 48.5, 24.3, 11.3 ppm; MS (m/z): 271 $[M+H]^+$; HRMS (TOF) calcd for $C_{15}H_{14}N_2O_3$: $[M+H]^+$, 271.1083; found, 271.1088.

*4.2.22. Synthesis of 7-hydroxy-2-(1-pentyl-1H-imidazol-5-yl)-4H-chromen-4-one (**10b**)*

Compound **10b** was prepared according to the procedure described for compound **8** starting from acetophenone **7** (0.56 g, 3.0 mmol) and compound **3b** (0.50 g, 3.0 mmol). The target compound **10b** (0.53 g) was obtained as white solid. Yield: 60.0%; mp: 191–192 ℃; IR (KBr, cm^{-1}) ν: 3457 (OH), 3057 (Ar–H), 1718 (C=O), 1625, 1546, 1481 (aromatic frame); ^{1}H NMR (600 MHz, DMSO-d_6) δ: 11.24 (s, 1H, O*H*), 7.89 (s, 1H, imidazole-2-*H*), 7.82 (s, 1H, imidazole-4-*H*), 7.58 (d, *J* = 8.4 Hz, 1H, flavone-5-*H*), 6.78 (d, *J* = 1.9 Hz, 1H, flavone-3-*H*), 6.70 (dd, *J* = 8.4, 1.9 Hz, 1H, flavone-6-*H*), 6.64 (s, 1H, flavone-8-*H*), 4.05 (t, *J* = 7.2 Hz, 2H, imidazole-CH_2), 1.77 (dt, *J* = 14.8, 7.4 Hz, 2H, CH_2), 1.31 (dt, *J* = 14.3, 7.2 Hz, 2H, CH_2), 1.23 (td, *J* = 8.0, 4.0 Hz, 2H, CH_2), 0.87 (t, *J* = 7.3 Hz, 3H, CH_3) ppm; ^{13}C NMR (151 MHz, DMSO-d_6) δ: 181.2, 167.7, 166.9, 146.2, 139.7, 129.5, 128.4, 126.0, 113.8, 113.4, 105.7, 99.0, 47.7, 30.7, 28.8, 23.5, 13.9 ppm; MS (m/z): 299 $[M+H]^+$; HRMS (TOF) calcd for $C_{17}H_{18}N_2O_3$: $[M+H]^+$, 299.1396; found, 299.1399.

*4.2.23. Synthesis of 2-(1-heptyl-1H-imidazol-5-yl)-7-hydroxy-4H-chromen-4-one (**10c**)*

Compound **10c** was prepared according to the procedure described for compound **8** starting from acetophenone **7** (0.56 g, 3.0 mmol) and compound **3c** (0.58 g, 3.0 mmol). The target compound **10c** (0.56 g) was obtained as white solid. Yield: 57.1%; mp: 111−113 ℃; IR (KBr, cm^{-1}) ν: 3443 (OH), 3030 (Ar–H), 1721 (C=O), 1632, 1540, 1497, 1458 (aromatic frame); ^{1}H NMR (600 MHz, DMSO-d_6) δ: 10.93 (s, 1H, O*H*), 7.91 (s, 1H, imidazole-2-*H*), 7.68 (s, 1H, imidazole-4-*H*), 7.53 (d, *J* = 8.1 Hz, 1H, flavone-5-*H*), 6.76 (d, *J* = 1.7 Hz, 1H, flavone-3-*H*), 6.54 (dd, *J* = 7.3, 2.5 Hz, 1H, flavone-6-*H*), 6.44 (s, 1H, flavone-8-*H*), 4.03 (t, *J* = 7.1 Hz, 2H, imidazole-CH_2), 1.84 (dt, *J* = 12.4, 8.1 Hz, 2H, CH_2), 1.30 (m, 8H, CH_2), 0.87 (t, *J* = 7.3 Hz, 3H, CH_3) ppm; ^{13}C NMR (151 MHz, DMSO-d_6) δ: 180.2, 168.7, 166.1, 149.9, 139.7, 129.5, 128.2, 126.0, 115.0, 114.2, 113.4, 101.7, 47.7, 31.8, 30.3, 29.3, 27.4, 22.4, 11.3 ppm; MS (m/z): 327 $[M+H]^+$. HRMS (TOF) calcd for $C_{19}H_{22}N_2O_3$: $[M+H]^+$, 327.1709; found, 327.1714.

*4.2.24. Synthesis of 2-(1-(3-chlorobenzyl)-1H-imidazol-4-yl)-7-hydroxy-4H-chromen-4-one (**11a**)*

Compound **11a** was prepared according to the procedure described for compound **8** starting from acetophenone **7** (0.56 g, 3.0 mmol) and compound **5a** (0.66 g, 3.0 mmol). The target compound **11a** (0.54 g) was obtained as white solid. Yield: 51.1%; mp: 167−168 ℃; IR (KBr, cm^{-1}) ν: 3443 (OH), 3030 (Ar–H), 1722 (C=O), 1626, 1541, 1493, 1458 (aromatic frame); ^{1}H NMR (600 MHz, DMSO-d_6) δ: 11.28 (s, 1H, O*H*), 8.13 (s, 1H, imidazole-2-*H*), 7.85 (s, 1H, imidazole-4-*H*), 7.57 (d, *J* = 8.4 Hz, 1H, flavone-5-*H*), 7.38 (dd, *J* = 18.0, 7.7 Hz, 2H, Ph-2,4-2*H*), 7.25 (s, 1H, Ph-5-*H*), 7.10 (d, *J* = 7.5 Hz, 1H, Ph-6-*H*), 6.83 (d, *J* = 1.9 Hz, 1H, flavone-3-*H*), 6.72 (dd, *J* = 8.5, 1.9 Hz, 1H, flavone-6-*H*), 6.69 (s, 1H, flavone-8-*H*), 5.55 (s, 2H, CH_2) ppm; ^{13}C NMR (151 MHz, DMSO-d_6) δ: 180.9, 167.2, 166.4, 146.7, 141.1, 140.2, 133.0, 131.6, 128.3, 127.5, 126.1, 125.9, 125.3, 113.3, 98.3, 96.1, 30.6, 30.5 ppm; MS (m/z): 353 $[M+H]^+$. HRMS (TOF) calcd for $C_{19}H_{13}ClN_2O_3$: $[M+H]^+$, 353.0693; found, 353.0694.

*4.2.25. Synthesis of 2-(1-(2,4-dichlorobenzyl)-1H-imidazol-4-yl)-7-hydroxy-4H-chromen-4-one (**11b**)*

Compound **11b** was prepared according to the procedure described for compound **8** starting from acetophenone **7** (0.93 g, 5.0 mmol) and compound **5b** (1.27 g, 5.0 mmol). The target compound **11b** (0.69 g) was obtained as white solid. Yield: 35.7%; mp: 181−182 ℃; IR (KBr, cm^{-1}) ν: 3421 (OH), 3015 (Ar–H), 1715 (C=O), 1629, 1543, 1488, 1462 (aromatic frame); ^{1}H NMR (600 MHz, DMSO-d_6) δ: 8.02 (s, 1H, O*H*), 7.85 (s, 1H, imidazole-2-*H*), 7.72 (s, 1H, imidazole-4-*H*), 7.54 (d, *J* = 6.9 Hz, 1H, flavone-5-*H*), 7.41 (d, *J* = 6.2 Hz, 1H, Ph-3-*H*), 6.77 (d, *J* = 54.8 Hz, 4H, Ph-5,6-2*H*, flavone-3,6-2*H*), 6.59 (s, 1H, flavone-8-*H*), 5.58 (s, 2H, CH_2) ppm; ^{13}C NMR (151 MHz, DMSO-d_6) δ: 180.8, 167.7, 166.9, 146.8, 141.8–141.7, 140.1, 134.0, 131.2, 128.2, 127.0, 126.1, 125.7, 125.4, 113.6, 99.2, 97.5, 49.0, 47.2 ppm; MS

(m/z): 387 $[M+H]^+$. HRMS (TOF) calcd for $C_{19}H_{12}Cl_2N_2O_3$: $[M+H]^+$, 387.0303; found, 387.0308.

*4.2.26. Synthesis of 2-(1-(4-chlorobenzyl)-1H-imidazol-4-yl)-7-hydroxy-4H-chromen-4-one (**11c**)*

Compound **11c** was prepared according to the procedure described for compound **8** starting from acetophenone **7** (0.93 g, 5.0 mmol) and compound **5c** (1.10 g, 5.0 mmol). The target compound **11c** (0.61 g) was obtained as white solid. Yield: 34.5%; mp: 171–172 ℃; IR (KBr, cm^{-1}) ν: 3450 (OH), 3028 (Ar–H), 1714 (C=O), 1635, 1540, 1477, 1458 (aromatic frame); ^{1}H NMR (600 MHz, DMSO-d_6) δ: 11.62 (s, 1H, O*H*), 9.08 (s, 1H, imidazole-2-*H*), 8.18 (s, 1H, imidazole-4-*H*), 7.60 (d, *J* = 8.5 Hz, 1H, flavone-5-*H*), 7.47 (d, *J* = 8.5 Hz, 2H, Ph-2,6-2*H*), 7.32 (d, *J* = 8.5 Hz, 2H, Ph-3,5-2*H*), 6.91 (d, *J* = 1.9 Hz, 1H, flavone-3-*H*), 6.77 (dd, *J* = 8.5, 1.9 Hz, 1H, flavone-6-*H*), 6.72 (s, 1H, flavone-8-*H*), 5.70 (s, 2H, CH_2) ppm; ^{13}C NMR (151 MHz, DMSO-d_6) δ: 180.6, 168.1, 167.7, 148.6, 139.0, 134.9, 133.4, 129.5, 126.4, 126.2, 113.9, 113.1, 99.4, 95.1, 48.5 ppm; MS (m/z): 353 $[M+H]^+$. HRMS (TOF) calcd for $C_{19}H_{13}ClN_2O_3$: $[M+H]^+$, 353.0693; found, 353.0701.

*4.2.27. Synthesis of 2-(1-(4-fluorobenzyl)-1H-imidazol-4-yl)-7-hydroxy-4H-chromen-4-one (**11d**)*

Compound **11d** was prepared according to the procedure described for compound **8** starting from acetophenone **7** (0.93 g, 5.0 mmol) and compound **5d** (1.02 g, 5.0 mmol). The target compound **11d** (0.65 g) was obtained as white solid. Yield: 38.5%; mp: 171–172 ℃; IR (KBr, cm^{-1}) ν: 3443 (OH), 3030 (Ar–H), 1720 (C=O), 1630, 1542, 1497, 1455 (aromatic frame); ^{1}H NMR (400 MHz, DMSO-d_6) δ: 11.38 (s, 1H, O*H*), 8.17 (s, 1H, imidazole-2-*H*), 7.96 (s, 1H, imidazole-5-*H*), 7.52 (d, *J* = 8.5 Hz, 1H, flavone-5-*H*), 7.41–7.36 (m, 2H, Ph-2,6-2H), 7.20–7.14 (m, 2H, Ph-3,5-2H), 6.77 (s, 1H, flavone-3-*H*), 6.67 (dd, *J* = 8.4, 1.9 Hz, 1H, flavone-6-*H*), 6.59 (s, 1H, flavone-8-*H*), 5.29 (s, 2H, CH_2) ppm; ^{13}C NMR (101 MHz, DMSO-d_6) δ: 181.1, 167.8, 167.0, 163.5, 161.1, 146.7, 139.0, 133.6, 133.0, 130.5, 126.2, 124.8, 116.2, 116.0, 113.6, 104.1, 99.0, 49.9 ppm; MS (m/z): 337 $[M+H]^+$; HRMS (TOF) calcd for $C_{19}H_{13}FN_2O_3$: $[M+H]^+$, 337.0988; found, 337.0984.

*4.2.28. Synthesis of 7-hydroxy-2-(1-(4-methoxybenzyl)-1H-imidazol-4-yl)-4H-chromen-4-one (**11e**)*

Compound **11e** was prepared according to the procedure described for compound **8** starting from acetophenone **7** (0.93 g, 5.0 mmol) and compound **5e** (1.09 g, 5.0 mmol). The target compound **11e** (0.41 g) was obtained as white solid. Yield: 23.5%; mp: 184–185 ℃; IR (KBr, cm^{-1}) ν: 3440 (OH), 3025 (Ar–H), 2944 (CH_3), 1715 (C=O), 1628, 1540, 1497, 1458 (aromatic frame); ^{1}H NMR (600 MHz, DMSO-d_6) δ: 8.05 (s, 1H, imidazole-2-*H*), 7.77 (s, 1H, imidazole-5-*H*), 7.50 (d, *J* = 8.5 Hz, 1H, flavone-5-*H*), 7.13 (d, *J*

= 8.7 Hz, 2H, Ph-2,6-2*H*), 6.92 (d, *J* = 8.7 Hz, 2H, Ph-3,5-2*H*), 6.70 (s, 1H, flavone-3-*H*), 6.63 (d, *J* = 6.4 Hz, 2H, flavone-6-*H*, flavone-8-*H*), 5.40 (s, 2H, CH_2), 3.71 (s, 3H, CH_3) ppm; ^{13}C NMR (151 MHz, DMSO-d_6) δ: 180.8, 168.2, 167.1, 164.5, 161.2, 146.1, 141.0, 132.3, 132.0, 131.0, 126.1, 125.9, 116.1, 115.5, 113.3, 104.4, 95.6, 55.4, 32.6 ppm; MS (m/z): 337 $[M+H]^+$; HRMS (TOF) calcd for $C_{20}H_{16}N_2O_4$: $[M+H]^+$, 337.0988; found, 337.0984.

*4.2.29. Synthesis of 2-(1-(3-chlorobenzyl)-1H-imidazol-5-yl)-7-hydroxy-4H-chromen-4-one (**12a**)*

Compound **12a** was prepared according to the procedure described for compound **8** starting from acetophenone **7** (0.93 g, 5.0 mmol) and compound **6a** (1.10 g, 5.0 mmol). The target compound **12a** (0.58 g) was obtained as white solid. Yield: 33.1%; mp: 163–164 ℃; IR (KBr, cm^{-1}) ν: 3422 (OH), 3025 (Ar–H), 1720 (C=O), 1629, 1540, 1497, 1455 (aromatic frame); ^{1}H NMR (600 MHz, DMSO-d_6) δ: 11.28 (s, 1H, O*H*), 8.13 (s, 1H, imidazole-2-*H*), 7.85 (s, 1H, imidazole-4-*H*), 7.57 (d, *J* = 8.4 Hz, 1H, flavone-5-*H*), 7.38 (dd, *J* = 18.0, 7.7 Hz, 2H, Ph-*H*), 7.25 (s, 1H, Ph-2-*H*), 7.10 (d, *J* = 7.5 Hz, 1H, Ph-*H*), 6.83 (d, *J* = 1.9 Hz, 1H, flavone-3-*H*), 6.72 (dd, *J* = 8.5, 1.9 Hz, 1H, flavone-6-*H*), 6.69 (s, 1H, flavone-8-*H*), 5.55 (s, 2H, CH_2) ppm; ^{13}C NMR (151 MHz, DMSO-d_6) δ: 180.9, 167.7, 166.3, 145.6, 142.3, 140.5, 134.5, 131.3, 128.8, 126.9, 126.0, 125.8, 125.1, 114.4, 98.5, 96.1, 30.5, 30.1 ppm; MS (m/z): 353 $[M+H]^+$; HRMS (TOF) calcd for $C_{19}H_{13}ClN_2O_3$: $[M+H]^+$, 353.0693; found, 353.0695.

*4.2.30. Synthesis of 2-(1-(2,4-dichlorobenzyl)-1H-imidazol-5-yl)-7-hydroxy-4H-chromen-4-one (**12b**)*

Compound **12b** was prepared according to the procedure described for compound **8** starting from acetophenone **7** (0.93 g, 5.0 mmol) and compound **6b** (1.27 g, 5.0 mmol). The target compound **12b** (0.63 g) was obtained as white solid. Yield: 32.7%; mp: 180–181 ℃; IR (KBr, cm^{-1}) ν: 3422 (OH), 3030 (Ar–H), 1721 (C=O), 1629, 1530, 1498, 1444 (aromatic frame); ^{1}H NMR (600 MHz, DMSO-d_6) δ: 11.44 (s, 1H, O*H*), 7.96–7.92 (m, 2H, imidazole-2-*H*, imidazole-4-*H*), 7.71 (d, *J* = 2.1 Hz, 1H, flavone-5-*H*), 7.58 (d, *J* = 8.4 Hz, 1H, Ph-3-*H*), 7.48 (dd, *J* = 8.4, 2.1 Hz, 1H, Ph-5-*H*), 7.17 (d, *J* = 8.4 Hz, 1H, Ph-6-*H*), 6.82 (d, *J* = 1.9 Hz, 1H, flavone-3-*H*), 6.74 (dd, *J* = 8.5, 1.9 Hz, 1H, flavone-6-*H*), 6.65 (s, 1H, flavone-8-*H*), 5.44 (s, 2H, CH_2) ppm. ^{13}C NMR (151 MHz, DMSO-d_6) δ: 181.2, 168.1, 166.8, 146.2–146.1, 139.3, 113.2, 106.2–106.1, 99.1–99.0, 46.9, 28.4, 14.3 ppm; MS (m/z): 387 $[M+H]^+$; HRMS (TOF) calcd for $C_{19}H_{12}Cl_2N_2O_3$: $[M+H]^+$, 387.0303; found, 387.0307.

*4.2.31. Synthesis of 2-(1-(4-chlorobenzyl)-1H-imidazol-5-yl)-7-hydroxy-4H-chromen-4-one (**12c**)*

Compound **12c** was prepared according to the procedure described for compound **8** starting from

acetophenone **7** (0.93 g, 5.0 mmol) and compound **6c** (1.10 g, 5.0 mmol). The target compound **12c** (0.55 g) was obtained as white solid. Yield: 31.3%; mp: 174–175 ℃; IR (KBr, cm^{-1}) ν: 3423 (OH), 3011 (Ar–H), 1723 (C=O), 1634, 1553, 1507, 1455 (aromatic frame); ^{1}H NMR (600 MHz, DMSO-d_6) δ: 7.93 (d, *J* = 7.8 Hz, 2H, imidazole-2-*H*, imidazole-4-*H*), 7.53 (d, *J* = 8.5 Hz, 1H, flavone-5-*H*), 7.45 (d, *J* = 8.4 Hz, 2H, Ph-2,6-2*H*), 7.36 (d, *J* = 8.4 Hz, 2H, Ph-3,5-2*H*), 6.69 (d, *J* = 1.6 Hz, 1H, flavone-3-*H*), 6.65 (dd, *J* = 8.5, 1.7 Hz, 1H, flavone-6-*H*), 6.59 (s, 1H, flavone-8-*H*), 5.33 (s, 2H, CH_2) ppm. ^{13}C NMR (151 MHz, DMSO-d_6) δ: 180.8, 168.7, 168.0, 146.5, 139.3, 136.8, 134.6, 133.0, 129.9, 129.2, 125.9, 124.6, 114.1, 112.8, 105.3, 98.8, 49.5 ppm; MS (m/z): 353 $[M+H]^+$; HRMS (TOF) calcd for $C_{19}H_{12}ClN_2O_3$: $[M+H]^+$, 353.0693; found, 353.0700.

*4.2.32. Synthesis of 2-(1-(4-fluorobenzyl)-1H-imidazol-5-yl)-7-hydroxy-4H-chromen-4-one (**12d**)*

Compound **12d** was prepared according to the procedure described for compound **8** starting from acetophenone **7** (0.93 g, 5.0 mmol) and compound **6d** (1.02 g, 5.0 mmol). The target compound **12d** (0.59 g) was obtained as white solid. Yield: 35.5%; mp: 170–171 ℃; IR (KBr, cm^{-1}) ν: 3440 (OH), 3030 (Ar–H), 1726 (C=O), 1629, 1556, 1499, 1458 (aromatic frame); ^{1}H NMR (400 MHz, DMSO-d_6) δ: 11.72 (s, 1H, O*H*), 9.43 (s, 1H, imidazole-2-*H*), 8.29 (s, 1H, imidazole-4-*H*), 7.60 (d, *J* = 8.5 Hz, 1H, flavone-5-*H*), 7.46–7.40 (m, 2H, Ph-2,6-2H), 7.29–7.22 (m, 2H, Ph-3,5-2H), 6.93 (d, *J* = 1.9 Hz, 1H, flavone-3-*H*), 6.81–6.75 (m, 2H, flavone-6-*H*, flavone-8-*H*), 5.74 (s, 2H, CH_2) ppm. ^{13}C NMR (101 MHz, DMSO-d_6) δ: 180.6, 168.2, 167.9, 163.6, 161.2, 149.2, 138.0, 131.5, 130.2, 126.6, 124.6, 116.5, 116.3, 114.1, 112.9, 99.5, 94.4, 49.0 ppm; MS (m/z): 337 $[M+H]^+$; HRMS (TOF) calcd for $C_{19}H_{12}FN_2O_3$: $[M+H]^+$, 337.0988; found, 337.0990.

*4.2.33. Synthesis of 7-hydroxy-2-(1-(4-methoxybenzyl)-1H-imidazol-5-yl)-4H-chromen-4-one (**12e**)*

Compound **12e** was prepared according to the procedure described for compound **8** starting from acetophenone **7** (0.93 g, 5.0 mmol) and compound **6e** (1.08 g, 5.0 mmol). The target compound **12e** (0.40 g) was obtained as white solid. Yield: 23.1%; mp: 172–173 ℃; IR (KBr, cm^{-1}) ν: 3426 (OH), 3035 (Ar–H), 2934 (CH_3), 1726 (C=O), 1626, 1548, 1479, 1458 (aromatic frame); ^{1}H NMR (600 MHz, DMSO-d_6) δ: 11.47 (s, 1H, O*H*), 7.94 (d, *J* = 15.2 Hz, 2H, imidazole-2-*H*, imidazole-5-*H*), 7.57 (d, *J* = 8.4 Hz, 1H, flavone-5-*H*), 7.33 (d, *J* = 8.7 Hz, 2H, Ph-2,6-2*H*), 6.95 (d, *J* = 8.7 Hz, 2H, Ph-3,5-2*H*), 6.87 (d, *J* = 1.9 Hz, 1H, flavone-3-*H*), 6.75 (dd, *J* = 8.4, 1.9 Hz, 1H, flavone-6-*H*), 6.64 (s, 1H, flavone-8-*H*), 5.25 (s, 2H, CH_2), 3.74 (s, 3H, CH_3) ppm; ^{13}C NMR (101 MHz, DMSO-d_6) δ: 181.2, 167.7, 166.9, 159.4, 146.2, 139.2, 134.2, 129.6, 126.0, 124.8, 114.6, 113.8, 113.4, 105.9, 98.9, 55.6, 49.9 ppm; MS (m/z): 349 $[M+H]^+$; HRMS (TOF)

calcd for $C_{20}H_{16}N_2O_4$: $[M+H]^+$, 349.1188; found, 349.1200.

*4.2.34. Synthesis of 7-hydroxy-2-(1H-imidazol-2-yl)-4H-chromen-4-one (**15**)*

Compound **15** was prepared according to the procedure described for compound **8** starting from acetophenone **7** (0.56 g, 3.0 mmol) and 1H-imidazole-2-carbaldehyde (0.29 g, 3.0 mmol). The target compound **15** (0.50 g) was obtained as white solid. Yield: 73.4%; mp: 170–171 ℃; IR (KBr, cm^{-1}) ν: 3400 (OH), 3019 (Ar–H), 2955 (CH_3), 1721 (C=O), 1628, 1550, 1483, 1452 (aromatic frame); ^{1}H NMR (400 MHz, DMSO-d_6) δ: 12.39 (s, 1H, O*H*), 7.61 (d, *J* = 8.4 Hz, 1H, flavone-5-*H*), 7.33 (m, 2H, imidazole-4,5-2*H*), 6.79 (s, 1H, flavone-3-*H*), 6.71 (d, *J* = 8.4 Hz, 1H, flavone-6-*H*), 6.60 (s, 1H, flavone-8-*H*) ppm; ^{13}C NMR (101 MHz, DMSO-d_6) δ: 181.4, 168.9, 167.1, 146.9, 140.2, 130.1, 126.4, 113.7, 113.3, 100.2, 99.1 ppm; MS (m/z): 229 $[M+H]^+$; HRMS (TOF) calcd for $C_{12}H_8N_2O_3$: $[M+H]^+$, 229.0613; found, 229.0616.

*4.2.35. Synthesis of 7-hydroxy-2-(1-propyl-1H-imidazol-2-yl)-4H-chromen-4-one (**16a**)*

Compound **16a** was prepared according to the procedure described for compound **8** starting from acetophenone **7** (0.56 g, 3.0 mmol) and **13a** (0.41 g, 3.0 mmol). The target compound **16a** (0.59 g) was obtained as white solid. Yield: 72.2%; mp: 167–168 ℃; IR (KBr, cm^{-1}) ν: 3422 (OH), 3032 (Ar–H), 2925 (CH_3), 1722 (C=O), 1628, 1555, 1480, 1451 (aromatic frame); ^{1}H NMR (400 MHz, DMSO-d_6) δ: 7.61 (d, *J* = 8.5 Hz, 1H, flavone-5-*H*), 7.43 (d, *J* = 0.9 Hz, 1H, imidazole-4-*H*), 7.22 (d, *J* = 0.7 Hz, 1H, imidazole-5-*H*), 6.78–6.63 (m, 3H, flavone-3-*H*, flavone-6-*H*, flavone-8-*H*), 4.15 (t, *J* = 7.1 Hz, 2H, imidazole-CH_2), 1.72 (dd, *J* = 14.4, 7.3 Hz, 2H, CH_2), 0.85 (t, *J* = 7.4 Hz, 3H, CH_3) ppm; ^{13}C NMR (101 MHz, DMSO-d_6) δ: 181.8, 168.9, 168.0, 147.8, 139.8, 131.1, 126.3, 123.7, 113.8, 112.7, 99.0, 96.7, 47.5, 24.7, 11.3 ppm; MS (m/z): 271 $[M+H]^+$; HRMS (TOF) calcd for $C_{15}H_{14}N_2O_3$: $[M+H]^+$, 271.1083; found, 271.1078.

*4.2.36. Synthesis of 7-hydroxy-2-(1-pentyl-1H-imidazol-2-yl)-4H-chromen-4-one (**16b**)*

Compound **16b** was prepared according to the procedure described for compound **8** starting from acetophenone **7** (0.56 g, 3.0 mmol) and **13b** (0.50 g, 3.0 mmol). The target compound **16b** (0.66 g) was obtained as white solid. Yield: 73.2%; mp: 163–163 ℃; IR (KBr, cm^{-1}) ν: 3431 (OH), 3025 (Ar–H), 2921 (CH_3), 1725 (C=O), 1627, 1600, 1466, 1452 (aromatic frame); ^{1}H NMR (400 MHz, DMSO-d_6) δ: 7.27 (d, *J* = 1.1 Hz, 1H, flavone-5-*H*), 7.12 (d, *J* = 8.9 Hz, 1H, imidazole-4-*H*), 7.07 (d, *J* = 1.1 Hz, 1H, imidazole-5-*H*), 6.18 (s, 1H, flavone-3-*H*), 5.94–5.90 (m, 1H, flavone-6-*H*), 5.73 (d, *J* = 1.8 Hz, 1H,

flavone-8-*H*), 4.07 (t, *J* = 7.1 Hz, 2H, imidazole-C*H*$_2$), 1.68 (dt, *J* = 14.5, 7.2 Hz, 2H, C*H*$_2$), 1.30 (dd, *J* = 15.1, 8.0 Hz, 2H, C*H*$_2$), 1.24–1.19 (m, 2H, C*H*$_2$), 0.85 (t, *J* = 7.1 Hz, 3H, C*H*$_3$) ppm; ^{13}C NMR (101 MHz, DMSO-d$_6$) δ: 182.3, 176.1–175.9, 151.3, 140.7, 129.9, 125.0, 122.1, 120.6, 103.2, 98.9, 91.0, 45.9, 31.0, 28.5, 22.0, 14.2 ppm; MS (m/z): 299 $[M+H]^+$; HRMS (TOF) calcd for $C_{17}H_{18}N_2O_3$: $[M+H]^+$, 299.1396; found, 299.1401.

*4.2.37. Synthesis of 2-(1-heptyl-1H-imidazol-2-yl)-7-hydroxy-4H-chromen-4-one (**16c**)*

Compound **16c** was prepared according to the procedure described for compound **8** starting from acetophenone **7** (0.56 g, 3.0 mmol) and **13c** (0.58 g, 3.0 mmol). The target compound **16c** (0.67 g) was obtained as white solid. Yield: 68.2%; mp: 169–170 °C; IR (KBr, cm^{-1}) ν: 3409 (OH), 3030 (Ar–H), 2935 (CH_3), 1721 (C=O), 1628, 1549, 1465, 1455 (aromatic frame); ^{1}H NMR (400 MHz, DMSO-d$_6$) δ: 7.55 (d, *J* = 8.5 Hz, 1H, flavone-5-*H*), 7.36 (d, *J* = 0.8 Hz, 1H, imidazole-4-*H*), 7.15 (d, *J* = 0.6 Hz, 1H, imidazole-5-*H*), 6.71 (d, *J* = 1.8 Hz, 1H, flavone-3-*H*), 6.66 (dd, *J* = 8.5, 1.9 Hz, 1H, flavone-6-*H*), 6.58 (s, 1H, flavone-8-*H*), 4.11 (t, *J* = 7.1 Hz, 2H, imidazole-C*H*$_2$), 1.62 (dd, *J* = 14.1, 7.1 Hz, 2H, C*H*$_2$), 1.22–1.10 (m, 8H, C*H*$_2$), 0.76 (t, *J* = 6.9 Hz, 3H, C*H*$_3$) ppm; ^{13}C NMR (101 MHz, DMSO-d$_6$) δ: 181.8, 168.8, 167.8, 147.7, 139.8, 131.2, 126.3, 123.7, 113.7, 113.1–112.9, 99.0, 96.8, 46.0, 31.6, 31.4, 28.5, 26.3, 22.4, 14.4 ppm; MS (m/z): 327 $[M+H]^+$. HRMS (TOF) calcd for $C_{19}H_{22}N_2O_3$: $[M+H]^+$, 327.1709; found, 327.1709.

*4.2.38. Synthesis of 2-(1-(3-chlorobenzyl)-1H-imidazol-2-yl)-7-hydroxy-4H-chromen-4-one (**17a**)*

Compound **17a** was prepared according to the procedure described for compound **8** starting from acetophenone **7** (0.56 g, 3.0 mmol) and **14a** (0.66 g, 3.0 mmol). The target compound **17a** (0.71 g) was obtained as white solid. Yield: 66.6%; mp: 169–170 °C; IR (KBr, cm^{-1}) ν: 3405 (OH), 3028 (Ar–H), 2931 (CH_3), 1724 (C=O), 1625, 1549, 1475, 1451 (aromatic frame); ^{1}H NMR (400 MHz, DMSO-d$_6$) δ: 7.39 (d, *J* = 1.1 Hz, 1H, flavone-5-*H*), 7.38–7.33 (m, 2H, Ph-2,4-2H), 7.16 (d, *J* = 1.0 Hz, 1H, imidazole-5-*H*), 7.09 – 7.02 (m, 2H, Ph-5,6-2H), 6.15 (s, 1H, imidazole-4-*H*), 5.88 (dd, *J* = 8.9, 1.8 Hz, 1H, flavone-3-*H*), 5.67 (d, *J* = 1.8 Hz, 1H, flavone-6-*H*), 5.43 (s, 1H, flavone-8-*H*), 5.29 (s, 2H, C*H*$_2$) ppm; ^{13}C NMR (101 MHz, DMSO-d$_6$) δ: 182.8, 170.5, 169.6, 154.4, 151.9, 141.1, 133.7, 131.0, 130.2, 129.0, 126.2, 125.0, 120.7, 105.1, 103.2, 98.9, 97.7, 90.6, 49.2 ppm; MS (m/z): 353 $[M+H]^+$. HRMS (TOF) calcd for $C_{19}H_{13}ClN_2O_3$: $[M+H]^+$, 353.0693; found, 353.0688.

*4.2.39. Synthesis of 2-(1-(2,4-dichlorobenzyl)-1H-imidazol-2-yl)-7-hydroxy-4H-chromen-4-one (**17b**)*

Compound **17b** was prepared according to the procedure described for compound **8** starting from acetophenone **7** (0.93 g, 5.0 mmol) and **14b** (1.27 g, 5.0 mmol). The target compound **17b** (1.42 g) was obtained as white solid. Yield: 73.2%; mp: 165–166 ℃; IR (KBr, cm^{-1}) ν: 3420 (OH), 3031 (Ar–H), 2931 (CH_3), 1728 (C=O), 1629, 1555, 1471, 1455 (aromatic frame); ^{1}H NMR (400 MHz, DMSO-d_6) δ: 7.44 (d, *J* = 1.8 Hz, 1H, flavone-5-*H*), 7.39 (d, *J* = 6.1 Hz, 1H, Ph-3-*H*), 7.15 (d, *J* = 1.2 Hz, 1H, imidazole-5-*H*), 6.77 (d, *J* = 54.8 Hz, 2H, Ph-5,6-2*H*), 6.13 (s, 1H, imidazole-4-*H*), 5.85 (dd, *J* = 8.6, 1.4 Hz, 1H, flavone-3-*H*), 5.62 (d, *J* = 1.4 Hz, 1H, flavone-6-*H*), 5.41 (s, 1H, flavone-8-*H*), 5.23 (s, 2H, CH_2) ppm; ^{13}C NMR (101 MHz, DMSO-d_6) δ: 181.5, 170.4, 168.8, 155.3, 152.0, 142.2, 133.8, 131.5, 130.3, 128.1, 126.3, 125.2, 120.8, 105.2, 103.1, 98.9, 97.5, 90.5, 49.1 ppm; MS (m/z): 387 $[M+H]^+$. HRMS (TOF) calcd for $C_{19}H_{12}Cl_2N_2O_3$: $[M+H]^+$, 387.0303; found, 387.0308.

*4.2.40. Synthesis of 2-(1-(4-chlorobenzyl)-1H-imidazol-2-yl)-7-hydroxy-4H-chromen-4-one (**17c**)*

Compound **17c** was prepared according to the procedure described for compound **8** starting from acetophenone **7** (0.93 g, 5.0 mmol) and **14c** (1.10 g, 5.0 mmol). The target compound **17c** (1.29 g) was obtained as white solid. Yield: 73.1%; mp: 169–170 ℃; IR (KBr, cm^{-1}) ν: 3423 (OH), 3044 (Ar–H), 2944 (CH_3), 1720 (C=O), 1630, 1571, 1473, 1452 (aromatic frame); ^{1}H NMR (400 MHz, DMSO-d_6) δ: 7.49 (d, *J* = 1.4 Hz, 1H, flavone-5-*H*), 7.20 (d, *J* = 2.2 Hz, 2H, Ph-2,6-2H), 7.18 (s, 2H, Ph-3,5-2H), 7.12 (d, *J* = 1.3 Hz, 1H, imidazole-5-*H*), 7.07 (d, *J* = 8.4 Hz, 1H, imidazole-4-*H*), 6.20 (s, 1H, flavone-3-*H*), 5.86 (dd, *J* = 8.4, 2.2 Hz, 1H, flavone-6-*H*), 5.65 (d, *J* = 1.9 Hz, 1H, flavone-8-*H*), 5.29 (s, 2H, CH_2) ppm; ^{13}C NMR (101 MHz, DMSO-d_6) δ: 181.7, 176.4, 172.4, 152.9, 142.6, 135.3, 132.2, 128.8, 124.1, 121.4, 114.6, 104.3, 97.6, 96.5, 91.6, 49.5 ppm; MS (m/z): 353 $[M+H]^+$. HRMS (TOF) calcd for $C_{19}H_{13}ClN_2O_3$: $[M+H]^+$, 353.0693; found, 353.0701.

*4.2.41. Synthesis of 2-(1-(4-fluorobenzyl)-1H-imidazol-2-yl)-7-hydroxy-4H-chromen-4-one (**17d**)*

Compound **17d** was prepared according to the procedure described for compound **8** starting from acetophenone **7** (0.93 g, 5.0 mmol) and **14d** (1.02 g, 5.0 mmol). The target compound **17d** (1.16 g) was obtained as white solid. Yield: 69.1%; mp: 164–165 ℃; IR (KBr, cm^{-1}) ν: 3325 (OH), 3031 (Ar–H), 2936 (CH_3), 1724 (C=O), 1625, 1539, 1471, 1455 (aromatic frame); ^{1}H NMR (400 MHz, DMSO-d_6) δ: 7.35 (d, *J* = 1.1 Hz, 1H, flavone-5-*H*), 7.19 (d, *J* = 2.8 Hz, 2H, Ph-2,6-2H), 7.17 (s, 2H, Ph-3,5-2H), 7.13 (d, *J* = 1.0 Hz, 1H, imidazole-5-*H*), 7.08 (d, *J* = 8.9 Hz, 1H, imidazole-4-*H*), 6.17 (s, 1H, flavone-3-*H*), 5.88 (dd, *J* =

8.1, 2.6 Hz, 1H, flavone-6-*H*), 5.68 (d, *J* = 1.8 Hz, 1H, flavone-8-*H*), 5.38 (s, 2H, C*H*$_2$) ppm; ^{13}C NMR (101 MHz, DMSO-d$_6$) δ: 182.7, 175.9, 170.5, 151.8, 141.5, 134.3, 130.2, 129.7, 125.0, 121.5, 115.9, 103.3, 98.9, 97.9, 90.8, 48.4 ppm; MS (m/z): 337 $[M+H]^+$; HRMS (TOF) calcd for $C_{19}H_{13}FN_2O_3$: $[M+H]^+$, 337.0988; found, 337.0990.

4.3. PTPs inhibition assay

The inhibitory effects and Kinetics analysis of the imidazole flavonoids against PTPs were measured similarly as described previously, using *p*-nitrophenol phosphate (*p*-NPP) as the substrate [30,31]. Briefly, the assays were performed on a 96-well plate in 20 mM MOPS buffer, pH 7.2, containing 50 mM NaCl. 10 μL of the compound at various concentrations was mixed with PTPs solution (82 μL) for 35 min at 37℃. Then 2 μL of *p*-NPP (0.1 M) substrate was added. After incubation for about 30 min, the assays were terminated by the addition of 6 μL of 2 M NaOH. The released *p*-nitrophenolate ion was determined by measuring the absorbance at 405 nm using microplate reader. The results of non-enzymatic hydrolysis of 2 μL *p*-NPP were compensated by measuring the control without enzyme addition. IC_{50} values were obtained by fitting the concentration-dependent inhibition curves using the Origin program (Origin Lab, Northampton, MA).

The inhibiting kinetic analysis was carried out according to the Lineweaver-Burk plot analysis. Phosphatase activities were measured at a fixed enzyme (PTP1B) concentration while concentrations of the substrate (*p*-NPP) and the inhibitor **11a** were varied. The data were fitted using Origin program to generate the Lineweaver-Burk plot.

The inhibiting kinetic analysis was performed according to rate equation (1)[32]:

$$v = \frac{V_{\max}[S]}{K_m\left\{1+\frac{[I]}{K_I}\right\}+[S]} \quad (1)$$

where V_{max} is the maximum initial velocity, K_m for Michaelis constant, [S] and [I] are concentrations of substrate and inhibitor, and K_i is the inhibition constant, derived from the slope of the Lineweaver–Burk plots.

The reaction rates of PTPs activity were determined in the absence and presence of fixed concentrations of inhibitor at a series of substrate concentrations. The reciprocal of the reaction rate was plotted as a function of the reciprocal of the substrate concentration for each concentration of inhibitor. The apparent Michaelis constant K_{app} values measured at the various inhibitor concentrations were plotted against concentrations of the inhibitor to calculate the inhibition constant K_i values.

*4.4. The influence of **11a** on cell viability*

The influence of **11a** on cell viability toward HEK293 cells was determined by using Cell Counting Kit-8 (CCK8, Yeasen Company) based on WST-8 (4-(3-(2-methoxy-4-nitrophenyl)-2-(4-nitrophenyl)-2H-tetraz-ol-3-ium-5-yl)benzene-1,3-disulfonate) reduction assay following literature procedures [33]. The HEK293 cells (5000 cells per well) were seeded into 96-well plates. The cells were then incubated in a culture medium containing compound **11a** with a particular concentration for 24 h. After that, 10 mL of CCK8 was added to each well. After 4 h, the unreacted dye was removed by aspiration. The OD values were spectrophotometrically measured in an ELISA plate reader (model 550, Bio-Rad) at a wavelength of 450 nm. The cell survival was expressed as follows: cell viability = (OD treated/OD control)×100%.

4.5. Molecular Docking

Molecular docking is a computational process of searching for a ligand that is able to fit both geometrically and energetically in the binding site of a protein. This is a process by which two molecules fit together in 3D space. The aim of protein−ligand docking is to predict the predominant binding model(s) for a ligand with a protein of known three-dimensional structure. AutoDock 4.2.3 is used for docking studies [34], and for internal conformational searches, autodock uses a Genetic Algorithm(GA) and a Lamarckian Genetic Algorithm to generate conformations [35].

Preparation of Protein and Ligand. The crystal structure of PTP1B (PDB ID: 1T4J) was obtained from the Protein Data Bank. 3D structure build of each flavonoid derivative ligand and the geometry optimization were through the ChemBioOffice 2014 software. In Autodock 4.2.3, water molecules and ions were removed (including ordered water molecules), and hydrogen atoms added at appropriate geometry groups within the protein were ionized as required at physiological pH. Functional groups in the structure of PTP1B were protonated in Autodock 4.2.3, which was chosen for docking studies, as this algorithm maintains the ligand flexibility and rigidity of PTP1B.

Docking Protocol. Macromolecule (PTP1B) and ligands (flavonoid derivatives) were opened in Autodock 4.2.3 software, which has been used widely because it shows acceptable free energy values relative to experimentally observed docking data [36]. To define all binding sites and to have structural inputs, a grid based procedure was used [37]. Here the output was saved as a PDBQT. The grid box was set, and the output was saved as a .gpf file. The ligand-centered maps were generated by the program AutoGrid with a spacing of 0.375 Å and dimensions of 60 × 60 × 60 points which was followed by blind docking [38]. All of the parameters were inserted at their default settings. In the docking tab, the macromolecule

and ligand are selected, and GA parameters are set as the number of GA runs: 50, population size: 150, maximum number of evals: 2 500 000, maximum number of generations: 27 000, maximum number of top individuals that automatically survive: 1, rate of genetic mutation: 0.02, rate of crossover: 0.8, GA crossover mode: two points, mean of Cauchy distribution for gene mutation: 0.0, variance of Cauchy distribution for gene mutation: 1.0, number of generations for picking worst individual: 10, output is selected as Lamarckian GA (4.2), and the file is saved as .dpf. The LGA was implemented in Autodock 4.2.3 to conduct docking simulations and to generate possible conformations of the drug binding in PTP1B. Among 50 conformations, the conformer with the lowest binding free energy should match with experimental data for further analysis.

4.6. Molecular Dynamics Simulations

A 50 ns MD simulation of the complex was carried out with the GROMACS 5.1.4 [39,40] using the GROMACS 96 force-field [41,42]. The initial conformation was chosen as the lowest binding energy docking conformation. The topology parameters of PTP1B were created by using the Gromacs program. The topology parameters of flavonoid derivatives were built by the Dundee PRODRG 2.5 server (beta) [43]. Then the complex was immersed in a dodecahedron box of extended simple point charge (SPC) water molecules. The solvated system was neutralized by adding sodium ions in the simulation, and the entire system was composed of 9152 atoms of PTP1B, one flavonoid derivative, 15 Na^+ counterions, and 94362 solvent atoms.

To release conflicting contacts, energy minimization was performed using the steepest descent method for 1000 steps, followed by the conjugate gradient method for 1000 steps. MD simulation studies consist of an equilibration and a production phase. In the first stage of equilibration, the solute protein, counterion, and flavonoid derivatives were fixed, and the position-restrained dynamics simulation of the system in which the atom positions of PTP1B were restrained at 300 K for 5 ns. Finally, the full system was subjected to 50 ns MD at a temperature of 300 K and 1 bar pressure [44]. The periodic boundary condition was used, and the motion equations were integrated by applying the Leapfrog algorithm with a time step of 2 fs. The atom coordinates were recorded every 10 ps during the simulation for latter analysis. The MD simulation and results analysis were performed on the Centos 7.0 Linux cluster with 18 nodes (dual Xeon processor).

Acknowledgments

This work was partially supported by Natural Science Foundation of the Jiangsu Higher Education Institutions of China (No. 17KJB150041), the practice inovation trainng program projects for the Jiangsu College students (No. 201710324004X, 201710324020Z, 201710324126C), the research open funding project of Jiangsu key laboratory for bioresources of saline soils (No. JKLBS2018008).

References

[1] (a) P. Punthasee, A.R. Laciak, A.H. Cummings, K.V. Ruddraraju, S.M. Lewis, R. Hillebrand, H. Singh, J.J. Tanner, K.S. Gates, Biochemistry, 56 (2017) 2051-2060; (b) R. Zhang, R. Yu, Q. Xu, X. Li, J. Luo, B. Jiang, L. Wang, S. Guo, N. Wu, D. Shi, Eur. J. Med. Chem., 134 (2017) 24-33.

[2] (a) R. Ottana, I. Adornato, P. Paoli, G. Lori, A. Nass, G. Wolber, V. Cardile, A. Graziano, E. Carol, A. Rotondo, R. Maccari, Eur. J. Med. Chem., 127 (2017) 840-858; (b) Y. Jia, C. Yuan, L. Lu, M. Zhu, S. Xing, X. Fu, Eur. J. Med. Chem., 128 (2017) 287-292.

[3] (a) C. Owen, E.K. Lees, N. Mody, M. Delibegovic, Diabetes Metab., 41 (2015) 95-101; (b) A.R. Saltiel, C.R. Kahn, Nature, 414 (2001) 799-806; (c) P. Heneberg, Curr. Med. Chem., 16 (2009) 706-733.

[4] A.P. Combs, W. Zhu, M.L. Crawley, B. Glass, P. Polam, R.B. Sparks, D. Modi, A. Takvorian, E. McLaughlin, E.W. Yue, Z. Wasserman, M. Bower, M. Wei, M. Rupar, P.J. Ala, B.M. Reid, D. Ellis, L. Gonneville, T. Emm, N. Taylor, S. Yeleswaram, Y. Li, R. Wynn, T.C. Burn, G. Hollis, P.C.C. Liu, B. Metcalf, J. Med. Chem., 49 (2006) 3774-3789.

[5] V.M. Balaramnavar, R. Srivastava, N. Rahuja, S. Gupta, A.K. Rawat, S. Varshney, H. Chandasana, Y.S. Chhonker, P.K. Doharey, S. Kumar, S. Gautam, S.P. Srivastava, R.S. Bhatta, J.K. Saxena, A.N. Gaikwad, A.K. Srivastava, A.K. Saxena, Eur. J. Med. Chem., 87 (2014) 578-594.

[6] T.N. Doman, S.L. McGovern, B.J. Witherbee, T.P. Kasten, R. Kurumbail, W.C. Stallings, D.T. Connolly, B.K. Shoichet, J. Med. Chem., 45 (2002) 2213-2221.

[7] (a) J.R. Beck, A. Lawrence, A.S. Tung, E.N. Harris, C.I. Stains, ACS Chem. Biol., 11 (2016) 284-290; (b) L.M. Scott, H.R. Lawrence, S.M. Sebti, N.J. Lawrence, J. Wu, Curr. Pharm. Des., 16 (2010) 1843-1862; (c) L.P. Lu, M.L. Zhu, Anti-Cancer Agents Med. Chem., 11 (2010) 164-171; (d) J. Luo, Q. Xu, B. Jiang, R. Zhang, X. Jia, X. Li, D. Shi, Selectivity, cell permeability and oral availability studies of novel bromophenol derivative HPN as protein tyrosine phosphatase 1B inhibitor. Brit. J. Pharmaco, 175 (2018) 140–153.

[8] P.H. Nguyena, T.T. Daoa, J. Kima, D.T. Phonga, D.T. Ndintehb, J.T. Mbaforc, W.K. Oh, Bioorg. Med. Chem., 19 (2011) 3378-3383.

[9] T.R. Helgren, R.J. Sciotti, P. Lee, S. Duffy, V.M. Avery, O. Igbinoba, M. Akoto, T.J. Hagen, Bioorg. Med. Chem. Lett., 25 (2015) 327-332.

[10] Farshid Zargari, Maryam Lotfi, Omolbanin Shahraki, Zahra Nikfarjam & Jafar Shahraki, J. Biomol. Struct. Dyn., 2017, 10.1080/07391102.2017.1409651.

[11] Y.H. Song, Z. Uddin, Y.M. Jin, Z. Li, M.J. Curtis-Long, K.D. Kim, J.K. Cho, K.H. Park, J. Enzyme Inhib. Med. Chem., 32 (2017) 1195-1202.

[12] H.A. Jung, P. Paudel, S.H. Seong, B.-S. Min, J.S. Choi, Bioorg. Med. Chem. Lett., 27 (2017) 2274-2280.

[13] (a) L. Zhang, X.M. Peng, G.L.V. Damu, R.X. Geng, C.H. Zhou, Med. Res. Rev., 34 (2014) 340-437; (b) X.M. Peng, G.X. Cai, C.H. Zhou, Curr. Top. Med. Chem., 13 (2013) 1963-2010.

[14] J.B. Liu, F.Q. Jiang, Y. Jin, Y. Zhang, J. Liu, W. Liu, L. Fu, Eur. J. Med. Chem., 57 (2012) 10-20.

[15] J.X. Ong, C.W. Yap, W.H. Ang, Inorg. Chem., 51 (2012) 12483-12492.

[16] I.Z. Gundhla, R.S. Walmsley, V. Ugirinema, N.O. Mnonopi, E. Hosten, R. Betz, C.L. Frost, Z.R. Tshentu, J. Inorg. Biochem., 145 (2015) 11-18.

[17] R. Luo, J. Wang, L. Zhao, N. Lu, Q. You, Q. Guo, Z. Li, Bioorg. Med. Chem. Lett., 24 (2014) 1334-1338.

[18] T.R. Helgren, R.J. Sciotti, P. Lee, S. Duffy, V.M. Avery, O. Igbinoba, M. Akoto, T.J. Hagen, Bioorg. Med. Chem. Lett., 25 (2015) 327-332.

[19] B.W. Li, F.H. Zhang, E. Serrao, H. Chen, T.W. Sanchez, L.M. Yang, N. Neamati, Y.T. Zheng, H. Wang, Y. Q. Long, Bioorg. Med. Chem., 22 (2014) 3146-3158.

[20] Y. Xie, W. Yang, F. Tang, X. Chen, L. Ren, Curr. Med. Chem., 22 (2015) 132-149.

[21] (a) L. Zhang, Y. Ge, H.M. Song, Q.M. Wang, C.H. Zhou, Bioorg. Chem., 80, (2018) 195-203; (b) L. Zhang, D. Addla, J. Ponmani, A. Wang, D. Xie, Y.N. Wang, S.L. Zhang, R.X. Geng, G.X. Cai, S. Li, C.H. Zhou, Eur. J. Med. Chem., 111 (2016) 160-182.

[22] L. Zhang, K.V. Kumar, S. Rasheed, R.X. Geng, C.H. Zhou, Chem. Bio. Drug Des., 86 (2015) 648-655.

[23] H.Z. Zhang, G.LV. Damu, G.X. Cai, C.H. Zhou, Eur. J. Med. Chem., 64 (2013) 329-344.

[24] S. Li, J.X. Chen, Q.X. Xiang, L.Q. Zhang, C.H. Zhou, J.Q. Xie, L. Yu, F.Z. Li, Eur. J. Med. Chem., 84 (2014) 677-686.

[25] S.F. Cui, D. Addla, C.H. Zhou, J. Med. Chem., 59 (2016) 4488-4510.

[26] W. Luo, Y. Chen, T. Wang, C. Hong, L.P. Chang, C.C. Chang, Y.C. Yang, S.Q. Xie, C.J. Wang, Bioorg. Med. Chem., 24 (2016) 672-680.

[27] Y.G. Zheng, M. Zheng, X. Ling, Y. Liu, Y.S. Xue, L.A., N. Gu, M. Jin, Bioorg. Med. Chem. Lett., 23 (2013) 3523-3530.

[28] E.P. Jesudason, S.K. Sridhar, E.J. Malar, P. Shanmugapandiyan, M. Inayathullah, V. Arul, D. Selvaraj, R. Jayakumar, Eur. J. Med. Chem., 44 (2009) 2307-2312.

[29] S.Q. Wen, P. Jeyakkumar, S.R. Avula, L. Zhang, C.H. Zhou, Bioorg. Med. Chem. Lett., 26 (2016) 2768-2773.

[30] (a) X.L. Li, T. Kurtán, J.C. Hu, A. Mándi, J. Li, X.W. Li, Y.W. Guo, J. Agric. Food Chem., 65 (2017) 1550-1555; (b) L. Ma, L.P. Lu, M.L. Zhu, Q.M. Wang, Y. Li, S. Xing, X.Q. Fu, Z.Q. Gao, Y.F. Dong, Dalton Trans., 40 (2011) 6532-6540.

[31] Q.M. Wang, L.P. Lu, C.X. Yuan, K. Pei, Z.W. Liu, M.L. Guo, M.L. Zhu, Chem. Commun., 46 (2010) 3547-3549.

[32] C.X.Yuan, L.P.Lu, X.L.Gao, Y.B.Wu, M.L.Guo, Y.Li, X.Q. Fu and M.L. Zhu, J. Biol. Inorg. Chem., 2009, 14, 841.

[33] J.E. Frith, D.J. Menzies, A.R. Cameron, P. Ghosh, D.L. Whitehead, S. Gronthos, A.C.W. Zannettino, J.J. Cooper-White, Biomaterials, 35 (2014) 1150-1162.

[34] G.M. Morris, R. Huey, W. Lindstrom, M.F. Sanner, R.K. Belew, D.S. Goodsell, A.J. Olson, J. Comput. Chem., 30 (2009) 2785-2791.

[35] G.M. Morris, D.S. Goodsell, R.S. Halliday, R. Huey, W.E. Hart, R.K. Belew, A.J. Olson, J. Comput. Chem., 19 (1998), 1639-1662.

[36] B. Gorelik, A. Goldblum, Proteins: Struct. Funct. Bioinf., 71 (2008) 1373-1386.

[37] P.J. Goodford, J. Med. Chem., 28 (1985) 849-857.

[38] C. Hetényi, D. van der Spoel, FEBS Lett., 580 (2006) 1447-1450.

[39] E. Lindahl, B. Hess, D. Van Der Spoel, Mol. Model. Annu., 7 (2001) 306-317.

[40] H.J.C. Berendsen, D. van der Spoel, R. van Drunen, Comput. Phys. Commun., 91 (1995) 43-56.

[41] W.R. Scott, P.H. Hu¨nenberger, I.G. Tironi, A.E. Mark, S.R. Billeter, J. Fennen, A.E. Torda, T. Huber, P. Krüger, W.F. van Gunsteren, J. Phys. Chem. A, 103 (1999) 3596-3607.

[42] L.D. Schuler, X. Daura, W.F. Van Gunsteren, J. Comput. Chem., 22 (2001) 1205-1218.

[43] A.W. Schuttelkopf, D.M. van Aalten, Acta Crystallogr., Sect D: Biol. Crystallogr., 60 (2004) 1355-1363.

[44] S. Jana, S. Dalapati, S. Ghosh, N. Guchhait, Biopolymers, 97 (2012) 766-777.

- ► Prepared imidazole flavonoids gave anti-PTP1B activity at the micromolar range.
- ► Compound **11a** (IC_{50} = 0.63 μM) displayed 9.5-fold selectivity for PTP1B over TCPTP.
- ► Cell viability assays indicated **11a** is cell permeable with lower cytotoxicity.
- ► Molecular modeling and dynamics studies revealed the reason of selectivity.

Identification of novel imidazole flavonoids as potent and selective inhibitors of protein tyrosine phosphatase

Ling Zhang[1,*], Yu Ge[1], Qing Ming Wang[1,*] and Cheng-He Zhou[2]

[1,*] *School of Pharmacy, Yancheng Teachers' University, Yancheng, Jiangsu 224051, People's Republic of China*

[2] *Laboratory of Bioorganic & Medicinal Chemistry, School of Chemistry and Chemical Engineering, Southwest University, Chongqing, 400715, P.R. China*

A series of novel active imidazole flavonoids were synthesized and evaluated as potential protein tyrosine phosphatase inhibitors. Further quantum chemical studies were evaluated to understand the structural features essential for activity.

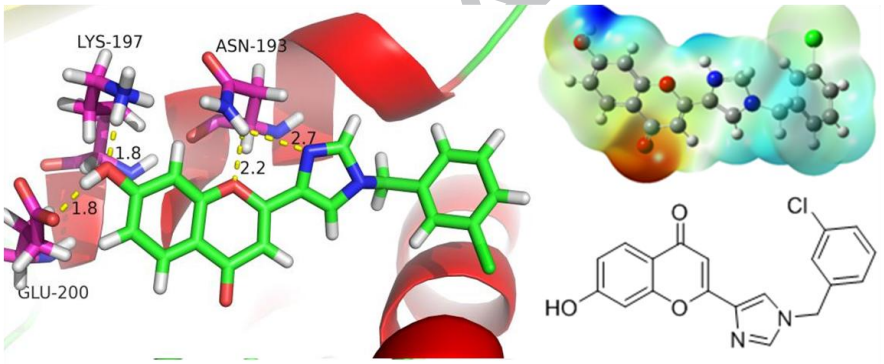

Binding energy = -8.78 kJ/mol

IC_{50} = 0.63 μmol/L